ADVANCED FUNCTIONAL MATERIALS
www.afm-journal.de

Integrative Approaches for DNA Sequence-Controlled Functional Materials

*Aaron Gadzekpo, Ewa Anna Oprzeska-Zingrebe, Mariana Kozlowska, Lennart Hilbert, and Iliya D. Stoev**

DNA carries a symbolic code that can be used to program the functional properties of DNA-based materials. Effective programming, however, requires the ability to predict how DNA sequence alterations modify emergent material properties, occurring at lengthscales a thousand to a million times larger than the base-pair level. This multiscale challenge can be addressed with integrative approaches that combine simulations, experiments and machine learning. This perspective article discusses how integrative approaches enable the characterization and design of functional materials composed of networks of DNA nanostructures with DNA-sequence-encoded interaction sites. Programmed at the base-pair level, these DNA nanomotifs impart complex sequence-property relationships by assembling into higher-order networks. State-of-the-art experimental and computational methods are presented for studying DNA nanomotif materials across scales. Furthermore, the potential of data-driven machine learning for transferring information between simulation scales is demonstrated, and its integration into iterative design strategies is discussed. Using DNA as a programmable building block, potential future applications are outlined in the form of biomimetic systems, mechanically tunable biomaterials, and information processing platforms.

1. Introduction

The relevance of DNA as an information carrier in living systems has long been established and inspired synthetic data storage solutions that encode information in the nucleotide sequence or in the shape of secondary structures.[1] The information stored in DNA sequences can also translate into material properties through the self-assembly of synthetic nanostructures driven by Watson–Crick base pairing and modulated by diverse macroscopic parameters, such as temperature and ionic strength.

Self-assembled DNA nanostructures can be grouped into two classes: mostly static 2D and 3D structures, formed by scaffolds and staple strands, and dynamic networks of interactive DNA particles in solution. The first class is well-known as DNA origami and was first proposed in the 1980s.[2] The goal of DNA origami is to generate stable shapes by folding and hybridization of DNA strands into a structure that minimizes the system's free energy.[3] DNA origami has been adapted for many applications, for example as synthetic membrane channels or as drug delivery platforms.[4,5] The second class of DNA nanostructures uses Watson–Crick base pairing to enable dynamic network formation between multivalent DNA molecules. In these systems, free energy minimization produces a viscoelastic network structure that is dynamic, allows for breaking and reforming of hydrogen bonds between DNA strands, and can withstand shear or extensional deformation. Building on pioneering work that established methods for assembling DNA nanomotifs into phase-separating, percolating networks,[6–8] more recent efforts focused on developing a new class of multifunctional programmable biomaterials. These dynamic DNA-based materials are now functionalized to respond to molecular, mechanical, thermal, or optical stimuli, enabling reconfigurable and adaptive behavior.[9] Recognizing their potential for diverse applications,[9–13] we focus this study on the second, dynamic class of DNA-based materials.

Dynamic networks of DNA molecules are typically assembled in a multi-step process, schematically depicted in **Figure 1**. First, using a heating cycle, commercially available single-stranded DNA oligomers (oligos) comprising tens of base pairs are annealed into DNA nanomotifs. These nanometer-sized motifs are also called nanostars due to their shape, and typically have three to six arms with single-stranded overhangs called "sticky ends". Sequence complementarity drives the assembly process to

A. Gadzekpo, E. A. Oprzeska-Zingrebe, L. Hilbert, I. D. Stoev
Institute of Biological and Chemical Systems - Biological Information Processing
Karlsruhe Institute of Technology
Hermann-von-Helmholtz-Platz 1, 76344 Eggenstein-Leopoldshafen, Germany
E-mail: iliya.stoev@kit.edu
M. Kozlowska
Institute of Nanotechnology
Karlsruhe Institute of Technology
Kaiserstraße 12, 76131 Karlsruhe, Germany

The ORCID identification number(s) for the author(s) of this article can be found under https://doi.org/10.1002/adfm.202519573

DOI: 10.1002/adfm.202519573

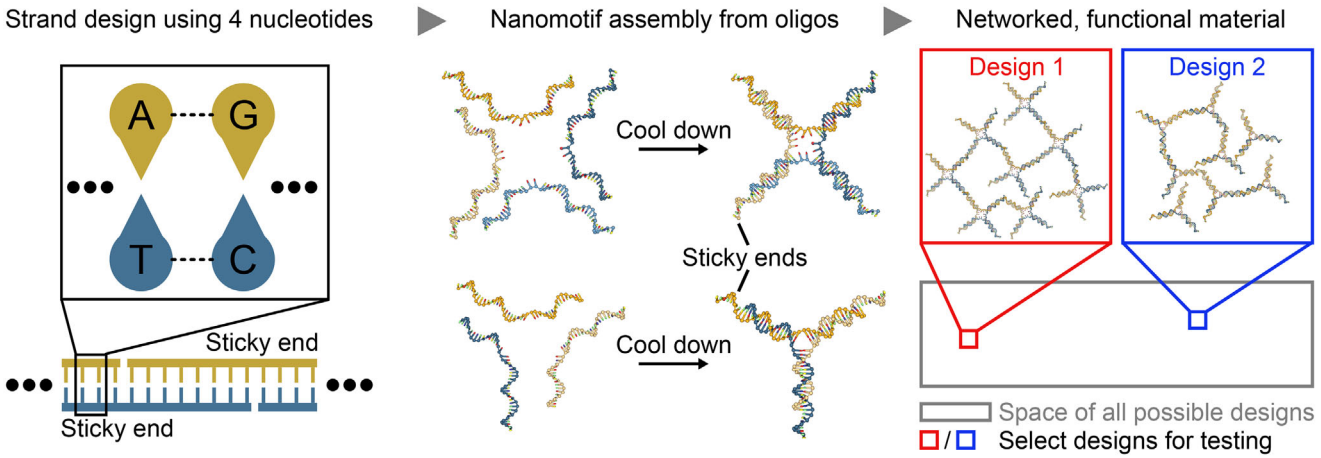

Figure 1. Designing materials composed of DNA nanomotifs. Starting at the level of base pairing, single strands of DNA are designed to hybridize into multivalent DNA nanomotifs. The single-stranded sticky end overhangs of the DNA nanomotifs facilitate assembly of higher-order networks comprising many DNA nanomotifs that are reversibly linked. To date, the large space of possible designs for functional materials has only been explored within narrow regions, exemplified by the two designs shown in the figure. Discovery and optimization of novel materials could be streamlined with scale-bridging methods, coupling the sequence information encoded in nucleotides to emerging network properties. Images of nanomotifs were generated with oxView.[14,15]

the most thermally stable configurations. The assembled DNA nanomotifs then form a networked material; the sticky ends of different nanomotifs hybridize to form a hydrogel with long-lived hydrogen bonds between motifs, or condensates with liquid-like properties and short-lived bonds. The network connectivity depends on the temperature, the level of electrostatic screening due to added salt ions, as well as the spatial DNA nanomotif structure, sequence, number and length of the sticky ends. Thus, the material properties are determined by the choice of DNA sequences, making the materials highly programmable.

In addition to their use in purely DNA-based materials, DNA nanomotifs can be fused with other additives or biomacromolecules, such as cholesterol or proteins, combining structural programmability with functional properties, such as molecular sensing, targeted delivery or catalysis.[16,17] Adding controlled reconfiguration, DNA strand displacement reactions can be used to exchange parts of the motif driven by an external cue, such as light, or addition of DNA oligomers.[18–20] The vast design space for nanomotif-based materials spans sub-nanosecond and nanometer scales when considering interactions between nucleotides, or seconds and millimeter scales when probing entire networks or hybrid materials. Different design subspaces enable emerging applications, such as biomimetic testbeds,[12] spatial control over chemical reactions,[19,21] or DNA-based computing.[10,11] Finding and optimizing nanomotif-based materials experimentally, based on a set of required properties and behavior, currently presents a bottleneck, as it involves time-consuming systematic testing of many parameters (e.g., sticky end sequence, temperature, DNA concentration). Reductions in synthesis costs have made custom orders of nanomole-scale quantities of short DNA oligomers, delivered dry or in ready-to-use stock solutions, relatively affordable. Libraries containing several (tens of) thousands of different sequences at nanomole synthesis scale, however, still remain prohibitively expensive. Additionally, DNA oligomers must be handled, combined in precise stoichiometric ratios, and undergo thermal annealing steps, followed by characterization with microscopes and rheometers, which in many cases are not set up for automated or high-throughput measurements. As a result, complete characterization may require weeks for a single design, making large-scale, brute-force screening of design libraries impractical. Moreover, local properties of DNA nanomotifs, such as melting temperatures of sticky ends that can be estimated with nearest-neighbor models,[22] couple to complex emergent mechanical and entropic effects at the level of nanomotifs and networks thereof, not captured by local models of DNA. As a result, many nanomotif designs are instead chosen ad hoc, without any clear rational motivation behind the choice of DNA sequences that gives rise to mesoscopic observables, such as rheological properties or phase behavior.

Addressing this challenge, our perspective article illustrates how simulations and experiments provide complementary insights into DNA nanomotif materials, spanning different timescales and lengthscales that can be combined to bridge the nucleotide-level strand design to emerging mesoscopic material properties. We showcase how method integration facilitated by machine learning (ML) aids in understanding bottom-up assembly of materials or streamline top-down design, toward prescribed properties and behavior. We begin with a brief introduction to atomistic and coarse-grained (CG) simulation methods for DNA structures (**Figure 2**A). Next, we discuss properties and behavior emerging on the scale of assembled nanomotifs and higher-order networks. In this context, we review how simulations can be used in conjunction with experiments that probe mesoscopic properties. Progressing to emerging and future directions, we briefly discuss advanced tools for passive and active microrheology, allowing systematic screening and spatial mechanical mapping of dynamic DNA nanomotif assemblies. Further, we outline and demonstrate a method that uses ML to transfer information accessible with nucleotide-level simulations onto a simplified CG model enabling the scaling-up and simulation of larger systems (Figure 2B–D). Leveraging data

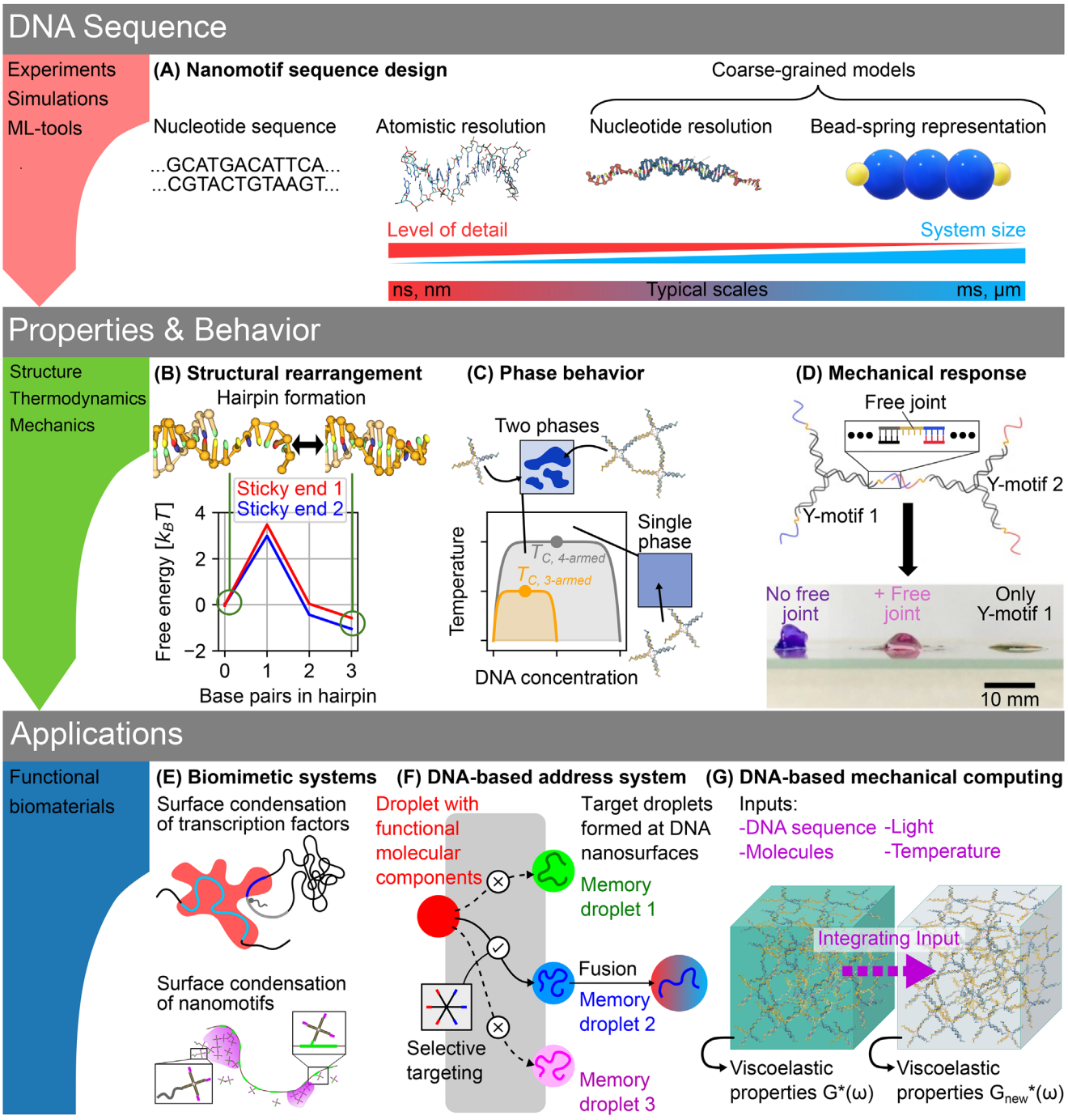

Figure 2. From nucleotides to functional materials. A) Functionality of DNA-based materials is encoded at the base-pair level. Simulations at different resolution in conjunction with experiments and machine learning (ML) allow to connect the design to emerging properties and behavior, which can be used for the discovery of new functional materials. Understanding how structural rearrangements within DNA segments B), as well as phase behavior C) and mechanical response D) of large DNA networks emerge from sequence design is crucial for enabling future applications. We expect that DNA will serve as a programmable building block for functional biomimetic materials that unveil key principles of cellular processes E), as an address system for targeted fusion of molecular payloads F), and for specialized mechanical computing, where networks of DNA nanomotifs integrate various input signals and output a measurable change in mechanical properties G). Images of nanomotifs at nucleotide level in (A), (B), (C) and (G) were generated with oxView.[14,15] Sketches in (E) adapted from ref. [13] under a CC BY license, Copyright 2025, the authors, published by Wiley Periodicals LLC. Schematic phase diagram in (C) based on experimental work in ref. [8]. Panel (D) reproduced with permission from ref. [23] under a CC BY-NC-ND license, Copyright 2018, the authors, published by the National Academy of Sciences.

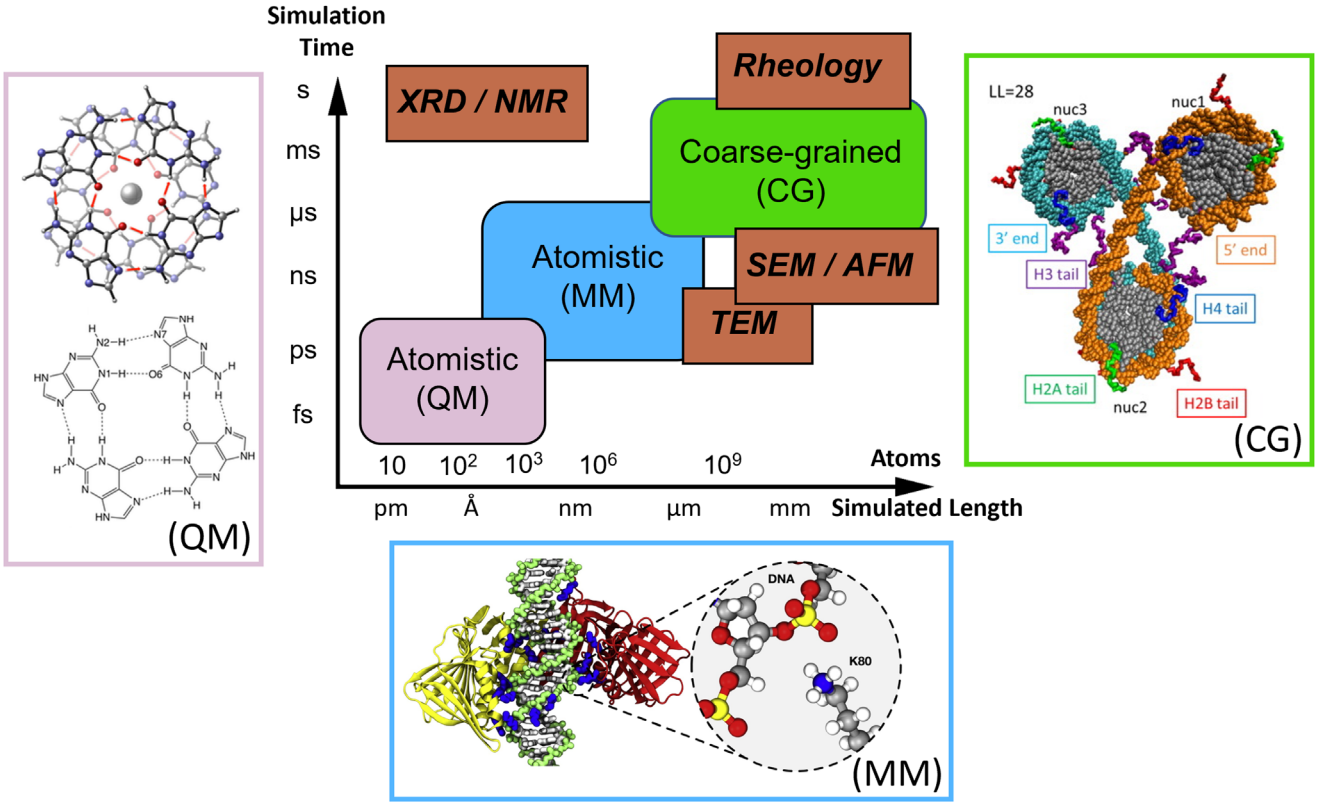

Figure 3. Representation of DNA systems calculated using different levels of theory. Length- and timescales apply to simulations, which can be validated with various experimental tools. Quantum mechanical (QM) calculations are used for understanding intricate and subtle interactions between atoms and reactivity of DNA fragments based on their electronic structure. Molecular mechanics (MM) using parameterized atomistic force fields (FF) can capture interactions between biological macromolecules and their conformational changes. Coarse-grained (CG) simulations represent molecular systems with lower resolution, allowing the simulation of larger systems over extended times. Inset figures represent (starting from the left): G-Quadruplex constituted of guanine tetrads (G4), held together by Hoogsteen-type hydrogen bonds,[27] all-atom model of a complex of proliferating cell nuclear antigen (PCNA) with DNA forming contact pairs between lysine and arginine residues at the PCNA-DNA interface,[28] and tri-nucleosome connected by two linker DNA segments with linker length (LL) of 28 base pairs.[29] These inset figures were reproduced with permission from: ref. [27] Copyright 2018, published by John Wiley and Sons; ref. [28] Copyright 2020, published by Elsevier; ref. [29] Copyright 2020, published by Elsevier.

containing sequence-property relationships, generated with such methods, we propose how ML could be used to solve the inverse problem of predicting designs based on a predefined set of requirements. To highlight the feasibility of integrative strategies that reliably connect material properties to underlying DNA sequence design, we review literature employing experimental and computational approaches to create and characterize DNA-based materials with diverse functionalities. Our aim is to show that many of the individual components of such integrative frameworks are already in place. We complement our discussion with relevant findings from fields, such as peptides and proteins, where ML methods have recently been successfully integrated into material design workflows. We close by describing promising applications enabled by the in-depth analysis of properties and behavior in biomimetic systems, spatial control of chemical reactions, and DNA-based computing (Figure 2E–G). Overall, we provide a detailed description of potential future directions and key milestones that must be reached to advance and transform the field toward targeted and knowledge-based development of sequence-controlled DNA-based functional materials.

2. Simulation Methods for DNA Across Scales

Simulation methods for DNA range from quantum mechanical treatment of few base pairs to CG models for kilobase pairs of DNA in chromatin or large-scale DNA origami. Consequently, there is considerable variation in the level of accessible detail, simulated timescales and lengthscales, as well as computational cost (**Figure 3**). In this section, we summarize simulation methods permitting the characterization of DNA sequence-encoded properties. Thus, methods resolving atoms, nucleotides and groups of nucleotides are considered. Simulations that incorporate the 3D structure of DNA and the thermodynamics of hybridization become essential for material design and characterization when local mechanical and thermodynamic features interact in non-trivial ways to produce emergent behavior. For instance, altering the number of nanomotif arms or modifying segment flexibility can lead to dramatic changes in viscoelastic responses, which cannot be predicted from sticky-end hybridization thermodynamics alone.[24,25] Furthermore, simulations are valuable in scenarios where non-equilibrium dynamics or interactions with other molecular components play a critical

role — factors that are often central to the function of DNA-based materials. This stands in contrast to routine applications, such as primer design, where local nearest-neighbor models[22] and tools, e.g., NUPACK,[26] are typically sufficient for accurate predictions. Multiscale modeling protocols provide insights into DNA-based biomaterials by linking the DNA sequence to properties of building blocks used to construct such materials, and by connecting those building blocks to properties and behavior emerging upon higher-order network formation.

2.1. Atomistic Simulations Offer Insights at Sub-Base-Pair Resolution

All-atom molecular dynamics (AA-MD) simulations have become an indispensable computational tool in molecular biophysics and biotechnology, providing detailed insights into the structural and dynamic properties of biomolecules on the atomic scale. They capture physical behavior on nanometer lengthscales and nanosecond timescales,[30] covering microseconds of simulated time using modern high-performance computing resources, such as Graphics Processing Unit (GPU) computing. This enables the study of complex biomolecular phenomena,[31–35] providing insights into the flexibility of DNA, its conformational folding transitions, and DNA-DNA or protein-DNA interactions.[28,36–38] Here, specialized all-atom-based force fields (FF) are typically used to describe interatomic interactions. Energetic contributions are evaluated by summing interactions between covalently bonded atoms (bonded terms) and long-range physical interactions (electrostatic and van der Waals forces). Frequently used force fields for AA-MD of DNA are iterations of the classic CHARMM[39] and AMBER[40] variants, including more recent parameter sets, e.g., OL21 and Tumuc1.[41,42]

In addition to regular AA-MD simulations that do not account for sampling bias, methods to upscale simulations through accelerated MD,[43] replica-exchange MD,[44] umbrella sampling,[45] and kinetic Monte Carlo[46] are in constant development.[47] Their application allows better understanding of processes that occur on long timescales or involve overcoming energy barriers. Due to their high degree of spatio-temporal resolution, all-atom simulations are particularly well-suited for investigating intricate mechanisms and interactions between DNA molecules that are challenging to observe through experimental methods alone.[48] Simulation output at atomistic resolution can be further used for the development of ML approaches that expedite large-scale simulations[49,50] or enable specific property prediction.[51,52] Another approach for lowering the computational cost of atomistic simulations following careful parameterization[53] is the implicit consideration of solvent, which renders the simulations more efficient,[54] though sacrificing information related to solvent-specific interactions.

Among the advantages of AA-MD is its synergistic coupling with even higher resolution simulation techniques, including quantum mechanical methods. Here, quantum mechanics/molecular mechanics (QM/MM) methods, especially in combination with implicit solvent models, can provide additional insights into microscopic phenomena or reactions involving DNA.[55] For example, such methods are widely used for simulating electron-transfer reactions,[56] reaction mechanisms[57,58] or for performing excited-state calculations with chromophores embedded in DNA.[59]

However, AA-MD simulations are limited in system size and simulated time (Figure 3). Modeling every atom within a large biomolecular system over biologically relevant timescales requires extensive computational resources and time, frequently constraining the simulations to microseconds. Therefore, simulating DNA with atomistic resolution is currently limited to hundreds of base pairs.[60] Insights into properties of single nanomotifs could thus still be derived at atomistic resolution - the nanomotifs shown in Figure 2C are comprised of 184 nucleotides. However, simulating the assembly of nanomotifs from single-stranded DNA and exploring how DNA sequence and hydrogen bond formation are linked with nanomotif topology and mechanical properties is accompanied with significant computational cost. For instance, one encounters such complexities during hairpin formation within palindromic sticky ends (Figure 2B). Furthermore, phenomena, such as phase-separation of DNA nanomotifs in solution (Figure 2C) or viscoelastic properties of hydrogels (Figure 2D), emerge at even longer timescales. Mechanical properties vary over many orders of magnitude in frequency[25] and phase-separated droplets experience constant internal rearrangements by dynamic breaking and re-forming of bonds between nanomotifs.[8,61] To investigate longer timescales and larger systems that exhibit the biophysics described above, one typically resorts to CG models.

2.2. Increasing System Size with Coarse-Grained Simulations

The upscaling of AA-MD simulations by using simplified molecular representations is a commonly used approach.[60,62] In CG simulations, atoms are grouped into larger spatial units, such as beads, thereby significantly reducing the degrees of freedom, and consequently gaining computational speed (Figures 2A and 3). The use of longer time steps enables extended simulation times and enlarged system sizes. The use of a continuous implicit solvent further lowers the computational cost. Customarily, a bottom-up approach is used to parametrize CG potentials from reference atomistic simulations. By virtue of statistical mechanics, the many-body Potential of Mean Force (PMF) for a given CG system is defined by the underlying atomistic model and the chosen CG scheme. Thus, parameters are often refined iteratively using pairwise PMFs with an additional fine-tuning to ensure closer match with experimental data. Force matching, relative entropy minimization or iterative Boltzmann inversion are alternatives to PMF.[63–65] Furthermore, interactions can be empirically parametrized, e.g., through a trial-and-error process, to align with experimentally observed thermodynamic properties, such as melting temperatures, or the structural and mechanical characteristics of double- and single-stranded DNA. Such top-down approaches were applied in popular CG models for DNA, viz., oxDNA[66,67] or 3SPN (Three-Site-Per-Nucleotide).[68] In general, the diverse properties of DNA across scales have led to the development of several CG FFs, each with a different focus. Overviews and detailed descriptions of CG models can be found elsewhere.[60,62,69] In the following text, we provide a short summary of two types of CG FFs that resolve nucleotides or groups of

nucleotides, making them suitable for efficiently and accurately simulating DNA nanomotifs.

The oxDNA force field is a state-of-the-art model that represents nucleotides as rigid bodies with interaction sites for base pairing, stacking interactions, and backbone connectivity.[67,70–73] The interaction potentials are designed to replicate base pairing and parametrized such that the mechanical response, hybridization and melting behavior of DNA are accurately reproduced. Recently, oxDNA was successfully used in many DNA nanotechnology and biophysics applications.[74–79]

oxDNA can be used as a standalone code with GPU optimization or via Large-Scale Atomic/Molecular Massively Parallel Simulator (LAMMPS)[80,81] implementation for both MD simulations and umbrella sampling. This combination makes oxDNA well-suited for investigating the behavior of single DNA nanomotifs, including sampling events that involve hybridization. As an example, Figure 2B shows the free energy profile of hairpin formation within a short DNA section that we obtained with umbrella sampling. Interestingly, sticky end sequence 2 (GCTCGAGC) had a lower free energy in a hairpin configuration compared to sticky end sequence 1 (CCACGTGG), when using a fully open state as a reference. Sticky end 2 would thus be more often found in a configuration that cannot hybridize with other sticky ends, possibly reducing the propensity for nanomotifs with this sticky end to phase separate.

Besides structural transitions within nanomotifs, even the assembly of nanomotif networks can be studied with oxDNA.[82] A limitation is that simulating relevant scales (≈100 nanomotifs, $\approx 10^9$ time steps) for a single design will require days of computing on current GPUs.[83] Therefore, further coarse-graining is practical for rapid testing of design parameters, as well as for sampling of emergent material features in more complex multi-component systems (e.g., interactive memory droplets, Section 4.2). Thus, models that approximate several base pairs as beads connected with springs are used to reduce the degrees of freedom, drastically accelerating simulations. Bead-spring models can be implemented using general-purpose MD software packages, such as LAMMPS or ReaDDy.[80,81,84] To preserve the physical validity of the obtained results, which may be otherwise hampered by omitting important atomic details, such bead-spring models can be parametrized by: 1) comparing relevant observables to higher-resolution models, 2) using methods from statistical physics to link parameters to existing knowledge, or 3) using ML to bridge between simulation scales.[85,86]

Together with atomistic simulations, CG simulations provide an important bridge from microscopic phenomena and processes to meso- and macroscopic observables accessible by experiments (Figure 3).

2.3. Applying Simulations in Synergy with Experiments

Here, we exemplify how computational and experimental results intersect, providing a combined, coherent picture of DNA structure formation, thermodynamics and mechanics.

Starting from the level of single molecules, MD simulations aid in the interpretation of results from single-molecule experiments, such as atomic force microscopy, optical tweezers or single-particle cryo electron microscopy (cryo-EM), for instance by explaining the angle-dependent response of DNA to shear stretching and the microscopic origins of structure and properties in DNA origami.[87–89] Moving to insights into molecular interactions, studies showed that specific base pairs create unique electrostatic environments within the minor groove, modulating how tightly tumor suppressor proteins bind DNA.[90–92] Other recent studies[93–95] demonstrated the sequence-dependent stability of G-quadruplex (G4) DNA structures and their potential as therapeutic targets, offering insights that are not readily accessible through experimental methods alone. Specifically, by capturing atomic-level interactions, such as hydrogen bonds and π-stacking between guanine bases, AA-MD simulations revealed the contribution of specific guanine tetrads and loop conformations to G4 thermal stability and response to mutations. These atomistic insights enabled researchers to predict the effects of single-nucleotide polymorphisms (SNPs) on the G4 structure, which may affect gene expression in oncogenes. Moreover, simulations complement experiments, such as circular dichroism (CD), nuclear magnetic resonance (NMR), electrophoretic mobility shift assays (EMSA) or mass spectrometry, which are used to develop therapies targeting G4 structures.[96,97] The importance of high-resolution details when modeling DNA was demonstrated in a study on the flexibility of DNA helices.[98] The authors compared AA simulations to a worm-like-chain polymer model, representing base pairs as beads. They found that parameterizing such a CG model for kilobase pair lengths underestimated the flexibility of short helices comprising 5 to 50 base pairs. They suggested that their findings could reconcile deviations in flexibilities found in experiments probing DNA strands of varied length.

Shifting focus to synthetic DNA nanostructures, a multi-step MD protocol was used to equilibrate a nanometer-sized DNA origami structure with atomistic resolution, in good agreement with a cryo-EM reconstruction of the same structure.[99] The authors further found that implicit treatment of the solvent in a model that uses elastic restraints between origami helices produced similar results at much-reduced computational cost. Cryo-EM of DNA nanostructures that mimic protein channels by forming a barrel-like structure, spanning a lipid bilayer, revealed that the nanostructure is dynamic, with at least five prominent conformations.[100] Simulations with a CG model of DNA[101] complemented this study by providing insights into the role of membrane pressure, salt concentration and the electrophysiological properties of the membrane-embedded structure.

On the micrometer scale, it was shown that the phase behavior and mechanical properties of a hydrogel comprising trivalent DNA nanomotifs linked by bivalent DNA linker strands can be tuned by making the linkers more flexible.[25] Nucleotide-level simulations using oxDNA were used to derive the probability distributions of angles between motif arms within the network, revealing that flexible bivalent linkers can bind two arms of the same motif. CG bead-spring models that include flexible or stiff bivalent linkers were then used to show that differences in the rheological response obtained from dynamic light scattering (DLS) experiments were, indeed, caused by the flexibility of the linkers. Similar models of trivalent DNA nanomotifs were also used in combination with confocal imaging of fluorescently labeled nanomotifs.[102] Here, the scaling between viscoelasticity and concentration in networks comprising building blocks of fixed valency was determined by emerging topological properties

on timescales shorter than the unbinding of nanomotif sticky ends. The possibility to add reconfiguration to DNA assemblies was explored with oxDNA, used to model the process of toehold-mediated strand displacement,[103,104] where a single strand of DNA is thermodynamically exchanged for another through highly selective branch migration. This approach has been used to control multi-compartment architectures made of DNA nanomotifs that mimic biological cells, sequential self-assembly found in nature and intracellular communication.[18,105,106]

To sum up, this overview highlights the synergistic link between simulations and experiments across scales, clearly indicating that deep integration will play a central role in the rational design of new functional biomaterials.

3. Integrative Tools for Scale-Bridging in the Development of DNA Nanomotif Materials

The deployment of DNA in functional materials is highly reliant on firm control of the phase behavior and material properties. Considering the vast design space, computational methods that connect the wide range of relevant scales hold great potential to significantly accelerate material discovery and optimization. The predictive power of simulations and ML methods, in turn, benefits from data-driven guidance through experimental quantification of DNA properties. Therefore, in this perspective, we focus on selected tools that enable efficient workflows for material design and characterization.

First, we discuss the use of simulations for screening of nanomotifs in combination with advanced experimental tools to connect designs with material properties. Following this, we showcase the use of Bayesian optimization for tuning simulation parameters across scales, connecting the design of nanomotifs with nucleotide properties. In the end, we conclude with an outlook on an integrated, ML-assisted workflow that streamlines the design of DNA-based nanomotif materials.

3.1. Accelerating Thermodynamic Studies of Phase Behavior and Mechanical Properties

Here we provide our perspective on the generation of an empirically informed database that links phase behavior and material properties to the DNA sequence design of nanomotifs, providing fundamental insights and facilitating progress in solving the inverse problem of mapping spatio-temporal properties back to starting DNA sequences.

DNA nanomotif networks exhibit mechanical properties that are strongly influenced by the valency, i.e., the number of arms per nanomotif.[24] Increasing the valency from three to six led to an increase in network stiffness and a transition in the concentration dependence of the elastic modulus from nonlinear to linear. This behavior was explained by the network approaching a Maxwell isostatic point, where junction constraints balance degrees of freedom, resulting in a shift from floppy, bending-dominated networks to rigid, stretch-dominated networks. Higher-valency networks showed reduced configurational freedom, diminished strain hardening, and lower extensibility, consistent with theoretical predictions for isostatic systems. Furthermore, the phase behavior of DNA nanomotifs was found to be highly temperature- and concentration-dependent.[8,61] The upper critical point in the consolution curves is directly influenced by nanomotif valency (Figure 2C), with a notable decrease in critical temperature and concentration as the valency is reduced. Assemblies of DNA nanomotifs with higher valency exhibit broader coexistence regions compared to those with lower valency.[8] Microrheology techniques point at a relationship between valency, composition and phase behavior.[20,23,25,107]

To harness this range of properties and behavior for functional materials, simulations can be employed in thorough screening of the phase behavior at a much-reduced cost, identifying designs that exhibit the desired emergent physics, for instance, forming microphase-separated droplets or a percolated hydrogel. Following this screening, passive and active microrheology tools can define the operating conditions of a prospective material through detailed investigation of the mechanical and thermodynamic properties.

Small-world rheology,[108] or microrheology, constitutes a wide range of scattering- or microscopy-based techniques, where the dynamics of a probe-particle or a tracer are linked via correlation functions to the material properties of a complex fluid using the generalized Stokes-Einstein relation (GSER):[109]

$$\tilde{G}(s) = \frac{k_B T}{\pi R s \widetilde{MSD}(s)} \tag{1}$$

where the complex viscoelastic modulus $\tilde{G}(s)$ in Laplace space depends on the Laplace frequency s, the thermal energy $k_B T$, the hydrodynamic radius of the tracers R, and the Laplace transform of the time-domain mean-squared displacement of the tracers $\widetilde{MSD}(s)$. This equation presents an important bridge between tracer particle dynamics and material properties of the medium in which the tracers are embedded. The GSER strictly holds true under conditions of equilibrium thermodynamics, pertinent to the state of many complex fluids away from a transition point.

Unlike standard UV-visible spectroscopy, microrheology techniques offer insights at high DNA concentrations where the Beer–Lambert law (linearly relating concentration and absorbance) fails. Compared to bulk rheology, microrheology operates across a broader frequency range, requires smaller samples, and provides localized rather than ensemble-averaged data. The microrheology tools, which characterize complex DNA systems that change their thermodynamic or mechanical state as a result of built-in responsiveness to stimuli, are broadly classified into passive and active. Passive techniques further divide into microscopy-based methods, e.g., multi-particle tracking[110,111] and simple single-beam optical tweezers,[112–114] and scattering-based methods, e.g., diffusing wave spectroscopy (DWS)[23,113] and DLS,[25,107] where the Brownian tracer dynamics are modeled as a random walk using an overdamped Langevin equation. Among these, DWS has been suggested as perhaps the most promising candidate tool for analyzing highly scattering media, such as highly concentrated DNA suspensions and hydrogel networks.[115,116]

In DWS, light propagation is represented as a random walk, where incident photons undergo multiple collisions with the tracer particles, and the material's viscoelastic characteristics are indirectly determined through particle dynamics, viz., the

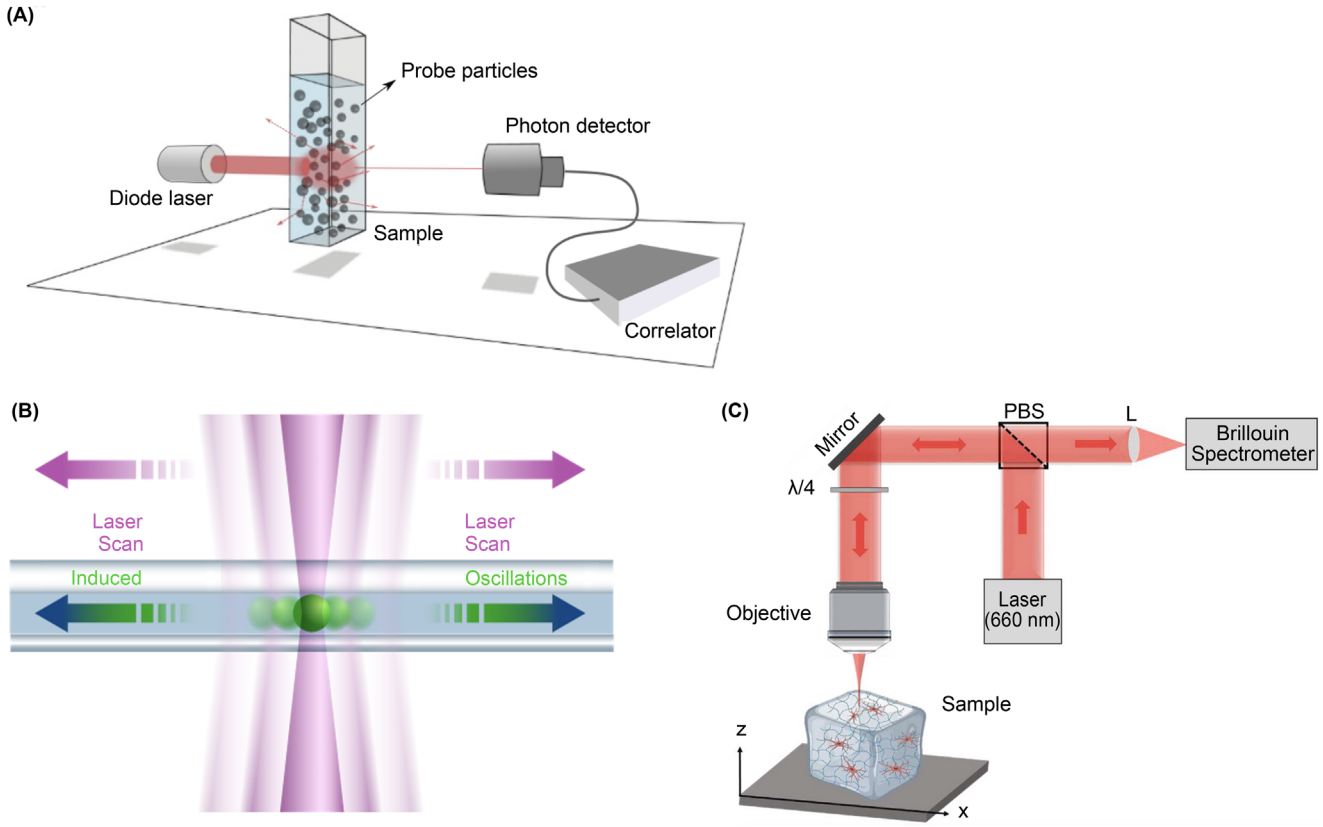

Figure 4. Microrheology methods for extraction of material properties. A) In passive DWS-based tools, intensity autocorrelations describe the dynamics of tracer particles and through the GSER provide a reliable route toward obtaining viscoelastic properties. B) Rheo-FLUCS is an active, phase-sensitive and probe-free microrheology tool that uses mild laser-induced temperature gradients to induce thermoviscous flows and measure the mechanical properties of living systems. C) Brillouin spectroscopy extracts mechanical information non-invasively at very high frequencies via the interaction between light and acoustic phonons, again without the requirement of introducing synthetic mechanical probes. Panel (A) reproduced with permission from ref. [23] under a CC BY-NC-ND license, Copyright 2018, the authors, published by the National Academy of Sciences. Panel (C) reproduced with permission from ref. [131], Copyright 2022, published by Elsevier.

mean-squared displacement (MSD) and intensity correlation function of the tracers (**Figure** 4A). Following application of the GSER and decomposing the complex viscoelastic modulus $\tilde{G}(s)$ into real and imaginary parts using Kramers–Kronig relations, one obtains information about the solid-like and liquid-like contributions of the gel network. Within the context of DNA hydrogels, relevant material parameters are the storage ($G'(\omega)$) and loss ($G''(\omega)$) moduli, whose relative magnitudes enable the determination of a temperature-dependent sol-gel transition. The latter reflects the melting temperature of the hydrogel's sticky ends, where on average half of all hydrogen bonds are formed or broken.

DWS measurements have so far provided important insights into the rigidity and elasticity of thermally activated DNA-based hydrogels, indicating that the network's mechanical robustness could be fine-tuned by altering structural elements like base-composition of the sticky ends[20] and insertion of flexible joints[25] between DNA building blocks. As highlighted by the distinct frequency response of the gel at different temperatures, these findings underscore the potential of DWS to sensitively track the mechanical state of DNA-based materials, facilitating the design of hydrogels with tailored properties.

More recently, high-throughput passive and active approaches based on Brillouin spectroscopy and focused light-induced cytoplasmic streaming (FLUCS) have been developed to multiplex mechanical measurements at different locations within samples from a set of diverse hydrogels, performing rapid screening of material properties and obtaining dynamic information in real time (Figure 4B,C).[117–119] This type of quick sweeps across the phase space often do not require the introduction of a mechanical probe, which renders them highly non-invasive and biocompatible, allowing the study of mechanical interplay between living cells and their embedding matrix, as well as the quick generation of material libraries to be subsequently used in ML algorithms as training datasets. Another alternative to conventional rheology is a recently developed micro-indenter which enabled rapid, small-volume characterization of DNA hydrogels by quantifying viscoelasticity and polymerization kinetics.[120]

Rheological measurements can also provide insights into non-equilibrium behavior during processes, such as network assembly, disassembly or reconfiguration. When probed on timescales much shorter than the material's relaxation time, non-equilibrium systems can often be approximated as quasi-equilibrium, enabling the use of equilibrium thermodynamic

principles. The onset of non-equilibrium dynamics can be investigated using established techniques, such as large-amplitude oscillatory shear (LAOS),[121,122] which captures non-linear viscoelastic responses, or through rapid, repeated scattering experiments. Additionally, ergodicity tests, comparing ensemble and time averages, can reveal deviations from equilibrium, particularly in glassy or gel-like states.[123] A common approach to quantify non-equilibrium phenomena and their deviation from equilibrium physics is the use of redefined, effective parameters, such as apparent temperature or apparent viscosity, which serve as proxies for non-equilibrium behavior.[124–126]

The integration of microrheology and sequence-aware simulations represents a promising route toward the rational design of DNA materials. Simulations can identify promising regions of the design space, steering experimental efforts away from brute-force screening and toward targeted exploration, while also providing microscopic insights that aid in interpreting rheological measurements. Together, these complementary strategies could enable predictive control over material properties and accelerate the development of DNA materials for application in areas, such as biocompatible computing, drug delivery, artificial tissue engineering and biosensing, which benefit from information about mesh size, relaxation times and thermal responsiveness.[9,127–130]

3.2. Bayesian Optimization for Tuning Coarse-Grained Force Field Parameters

In this section, we describe how ML techniques can transfer information accessible only at or below nucleotide resolution to models that simplify the representation of DNA by further coarse-graining. These optimized CG models allow for efficient exploration of the design space of DNA-based materials. In other words, the goal of this strategy is to model DNA nanomotifs in a way that is sequence-aware but simplified enough to scale simulations to larger systems that exhibit emergent macroscopic behavior.

At a high level, the algorithm uses ML to propose parameters for a bead-spring ("microscale") model of DNA nanomotifs. These parameters are evaluated through microscale simulations, where the outcomes are compared against a nucleotide-level ("nanoscale") reference. Based on the similarity between micro- and nanoscale simulations, the ML model is updated. This process is repeated until the microscale model reliably reproduces the sequence-dependent behavior of the nanoscale system. **Figure** 5A provides a graphical summary of an exemplary workflow that uses oxDNA to generate a nucleotide-resolution reference for the structure of X-shaped DNA nanomotifs. Structural information is then transferred to a simplified bead-spring model implemented in ReaDDy, which can be used to simulate larger networks of nanomotifs over longer time.

Concretely, structural information of DNA nanomotifs (Figure 5B–F) was captured with oxDNA simulations, providing target nanoscale observables. To this end, vectors were aligned to groups of nucleotides, defining six angle distributions with analogs in a microscale bead-spring model (Figure 5G). In this bead-spring model, volume exclusion and harmonic bond potentials between beads were fixed prior to optimization, leaving eight angle potential parameters to capture the flexibility of the nanomotif. This choice also reflects the fact that measurements of persistence length, which are linked to an angle potential, showed strong dependence on temperature, salt concentration and strand length.[98,133,134]

We developed Python code that automates the optimization of simulation parameters via ML. In the example shown here, a Gaussian process modeled the relationship between bead-spring parameters and fitness defined by similarity between angle distributions from both simulation scales.

Fitness was iteratively optimized with Bayesian optimization, chosen due to its capability of handling complex fitness functions and high-dimensional search spaces, without requiring a large training dataset.[135] The application of Bayesian optimization in the parameter tuning of CG polymer models has recently been demonstrated.[86] For efficiency and state-of-the-art capabilities, Bayesian optimization with a Gaussian process was implemented using the BoTorch library, which is based on PyTorch.[136,137] The algorithm is designed to integrate with any simulation framework whose fitness can be retrieved through a Python function. Importantly, in our implementation the algorithm can simultaneously use independent Gaussian processes for independent sets of parameters. This way, parts of a molecule (for instance, the sticky ends of a nanomotif) that do not interact strongly with other parts (for instance, the center of the nanomotif) can be optimized using the same set of trial simulations. In its current implementation we observed convergence of fitness after ≈200 trial simulations, which is distinctly more efficient than a brute force approach which would require $\approx 10^4$ simulations if 10 values were tested for each parameter, due to the coupled angles in Figures 5C,D. For most angle distributions (Figures 5B,C,E), a close match between simulation scales was observed, while some persisting deviations (Figure 5D) indicated that the much simpler bead-spring model was unable to reproduce all structural detail resolved in the nucleotide model.

This approach illustrates the efficiency of an ML framework to automate simulation parameter optimization by comparing observables from a simplified but scalable simulation to a target reference from a highly detailed but expensive simulation. Such a computational workflow addresses a current bottleneck of simulation-aided design, viz., the need to update model design and parametrization with each change to nanomotif sequence and external control parameters. We plan to validate this approach further, e.g., with CG models for 3-armed nanomotifs and by modulating the repulsion between arms by changing the salt concentration. Experimental observations, such as mechanical response measured with diffusing wave spectroscopy or Rheo-FLUCS, could be included into the fitness by simulating and evaluating a network of motifs (Figure 5H). Furthermore, different optimization schemes, acquisition and fitness functions will be explored in the future.

A crucial question relates to scalability and reliability of CG models. Any simulation will have limitations depending on the level of included details, thus the degree of coarse-graining has to be tuned to balance computational efficiency and predictive accuracy, enabling simulations across a wide range of system sizes (Figure 2A). Current CG models, while typically not sequence-aware, allowed simulations of hundreds to thousands of DNA nanomotifs and reliably captured trends, scaling and general bulk behavior observed in experiments.[12,25,102,138,139]

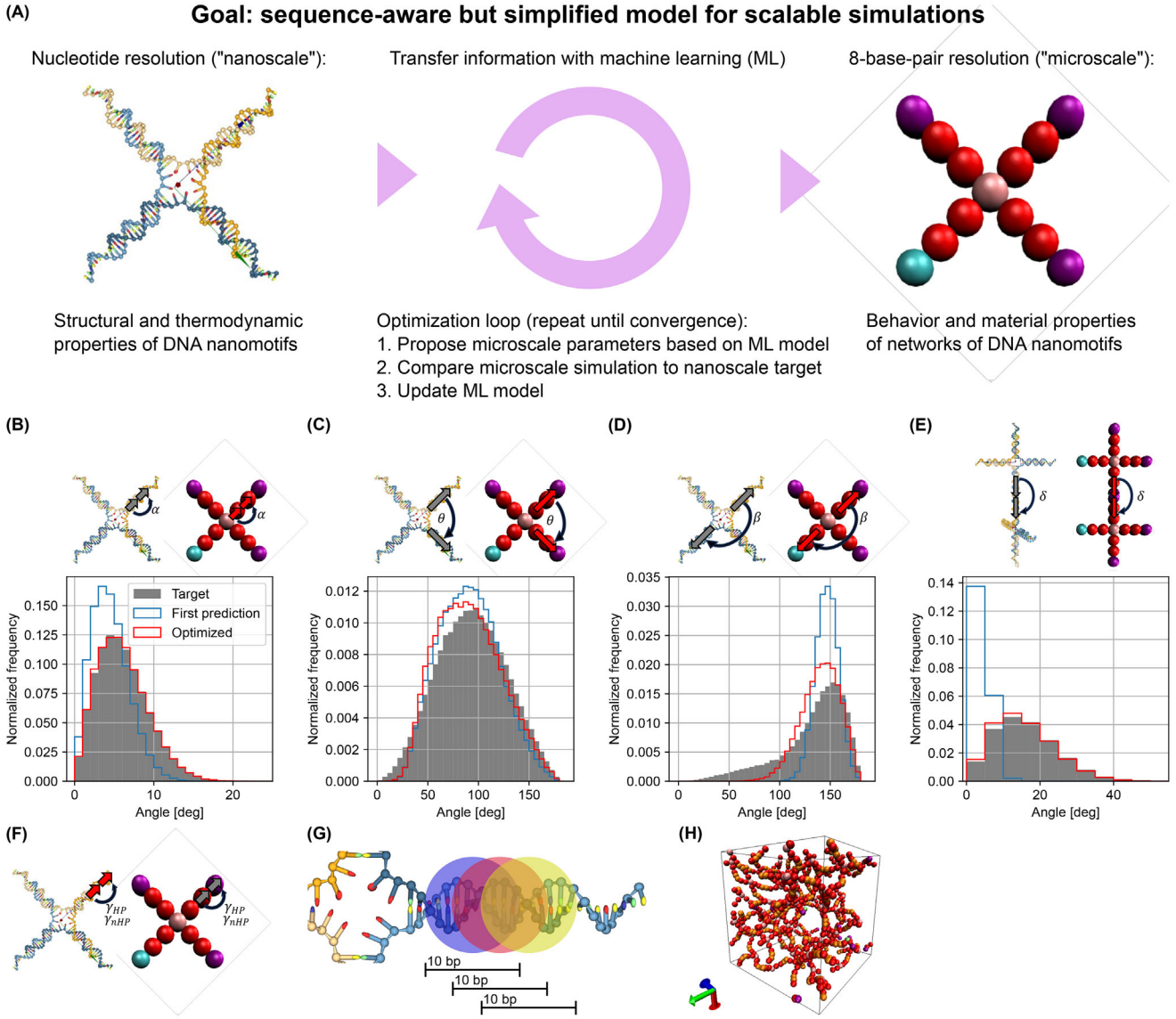

Figure 5. Information transfer across scales with iterative machine learning. A) The goal of the algorithm is to tune parameters in a CG microscale model, such that the model approximates nanoscale target observables. The algorithm requires target observables, e.g., angle distributions from a high-resolution nanoscale simulation, and a set of tuneable parameters for the CG microscale model. Each iteration of ML-guided optimization starts with a proposed parameter set for the microscale model, followed by trial simulations that are compared to the nanoscale target and used to update the ML model. Here, the implementation employed Bayesian optimization with a Gaussian process model, not excluding the use of other schemes. B–E) Angles within and between nanomotif arms were optimized. Target angle distributions, as well as distributions from first and optimal predictions, are shown. Optimization of single spring constants in A and D converged after ≈15–25 iterations, the four coupled parameters (equilibrium angles and spring constants) in B and C required ≈100 iterations. F) The angle involving the sticky ends with or without hairpin was also optimized (data not shown). G) Groups of ten base pairs were used to define coordinate centers to align vectors for angle evaluation. Here we show the angle within arms from panel A. H) The optimized model can be used to simulate large network of nanomotifs. Details of model parameters, the implementation of simulations and the ML strategy can be found on GitHub, where we prepared Jupyter notebooks to run the workflow, providing an extensible toolbox to the community. Images of nanomotifs at nucleotide level generated with oxView,[14,15] bead-spring model visualized with VMD.[132]

Furthermore, implementing CG models with general MD software, such as LAMMPS and ReaDDy, facilitates studies of heterogeneous or multi-component DNA materials. Beyond DNA materials, scale-bridging frameworks demonstrated strategies to overcome limitations of coarse-graining: atomistic-to-mesoscale models have captured chromatin organization in systems exceeding 1000 nucleosomes, while scale-bridging ML-driven and hybrid approaches have been applied to biological membranes and organic electronic devices, suggesting similar scalability for complex DNA-based architectures.[140–142] Ultimately, experimental validation remains essential to assess how these strategies perform at larger scales, highlighting the benefits of integrating ML and simulation-guided design with targeted experiments.

While optimized simulations and tools, such as DWS or RheoFLUCS, solve the forward problem of linking DNA sequence design to material properties, the inverse problem could be solved with a training dataset sufficiently large for application of ML for sequence-property decoding.

3.3. Machine Learning for Efficient Design of DNA-Based Materials

Data-driven science has also been called the "4th paradigm," building on the three preceding paradigms of empirical, theoretical and computational sciences.[143,144] It has led to breakthroughs in areas, such as inverse design of high-performing solar cells,[145] as well as autonomous design and analysis of proteins with targeted mechanical properties,[146] and we expect similar impact in the field of functional DNA-based materials. However, solving the inverse problem of sequence-level programming of DNA for functional materials has not been reported yet. To address this gap, we envision that suitable methods could integrate information from experimental and computational approaches, enabling data-driven navigation of the vast design space,[143,144] while performing targeted experimental validation of markedly different regions, i.e., "islands" within this design space.

First, simulations with CG models, discussed in Section 2.2, are used for inexpensive screening of the design space: for instance, by simulating a section of the bulk material, e.g., ≈ 100 nanomotifs in a periodic box, and varying the number, length and flexibility of nanomotif arms, the sequence of the sticky ends and external parameters, such as temperature or salt concentration. In this way, material properties, such as the complex shear modulus, network connectivity, saturation concentration etc. could be estimated based on behavior of molecules and networks in the simulations. ML can connect the CG model parameters with validated DNA properties by parameter optimization, as described in Section 3.2. The initial screening is used as a training dataset for a predictive ML algorithm that learns to connect nanomotif sequence design with emerging material features. This dataset is then augmented and validated with experiments for selected design regions (e.g., those with high uncertainties, sparse sampling or theoretical promise beyond known material boundaries). During inference, the ML algorithm is employed in design predictions (**Figure 6**). Starting with a list of requirements, the algorithm proposes promising design sub-spaces for further exploration with simulations and experiments that are then iteratively added to the training dataset in a process of continuous improvement and refinement. Such an active learning strategy could navigate the complex design space toward suitable sub-spaces, while maintaining the connection to validated nucleotide-level properties.

A necessary step before training such a model is defining a representation of the inputs and outputs that describes a DNA nanomotif-based material. As an example, the input could be a feature vector containing desired material properties, such as viscoelastic properties or saturation concentrations. The output might summarize bulk concentrations, temperature, and the number and length of nanomotif arms for a high-level representation. At a lower level, a graph representation of the nanomotif structure, resolved at different levels of coarse-graining, could be suitable. Nodes and edges then encode binding energies of sticky ends or mechanical properties within or between motif arms. Such a model is then trained on a library containing the observed material properties as well as the material design. Suitable ML model architectures will have to handle the discrete nature of the DNA sequence and building block properties, such as the number of arms with sticky ends, but also continuous variables, such as temperature and bulk concentrations.

A technique of particular interest here is Bayesian optimization, which is capable of modeling complex input-output relationships, while often requiring only ≈10 to 100 datasets to navigate the design space.[147–149] Since sequence input is the basis of DNA materials, other natural choices are recurrent neural networks or transformer architectures. While these architectures require a larger training dataset, application could benefit from existing foundation models.[150–152] Bridging physics and "black box" ML to achieve reliable, generalizable models for material design also requires physics-informed models, embedding fundamental constraints into learning algorithms, hybrid frameworks coupling simulations with ML, and interpretable AI approaches.[153–155] Another interesting avenue is the use of large language models to distill findings of existing publications, thus generating a database.[156] Applied to peptide self-assembly, data mining from literature, dataset curation, and prediction of self-assembly phases based on sequence and conditions have been demonstrated.[157] For protein-based materials, which also have complex sequence-property relationships, recent developments in multi-agent systems have shown success in autonomously discovering design principles. Frameworks, such as Sparks,[158] ProtAgents,[146] and SciAgents,[159] combine large language models, physics-based simulations, and graph reasoning to generate hypotheses, design proteins with desired mechanical properties, and uncover new structure-function relationships. The use of graph-based reasoning and agent collaboration could offer a scalable approach to exploring the vast combinatorial space of DNA nanomotifs and their assemblies. Crucially, ML for material design is broadly applicable across a wide spectrum of material classes, such as organic molecules, polymers, catalysts, alloys, semiconductors, battery materials, and porous materials.[160–163] Guidance by such previous work will expedite application to DNA materials.

To further illustrate the potential of targeted sequence-programming in networked materials, we refer to previous demonstrations of sequence-property relations, as well as ML-guided expansion of a material property space. A study that used DNA hydrogels produced via Rolling Circle Amplification (RCA) revealed that systematic screening of experimental conditions and template sequence affected RCA yield as well as mechanical properties of the hydrogels.[164] DNA-cross-linked materials with programmable viscoelasticity enabled tunable stress relaxation for cell and organoid culture,[165] while sequence-directed hybridization cascades drove shape changes in photopatterned hydrogels via controlled swelling.[166] Bayesian optimization of hydrogels comprising acrylic and methacrylic components has extended the space of observable properties related to the photodegradability of a hydrogel.[167]

Many individual components for integrated workflows are already established. The adoption of standardized protocols, rigorous benchmarking, open-source tools, and the continued

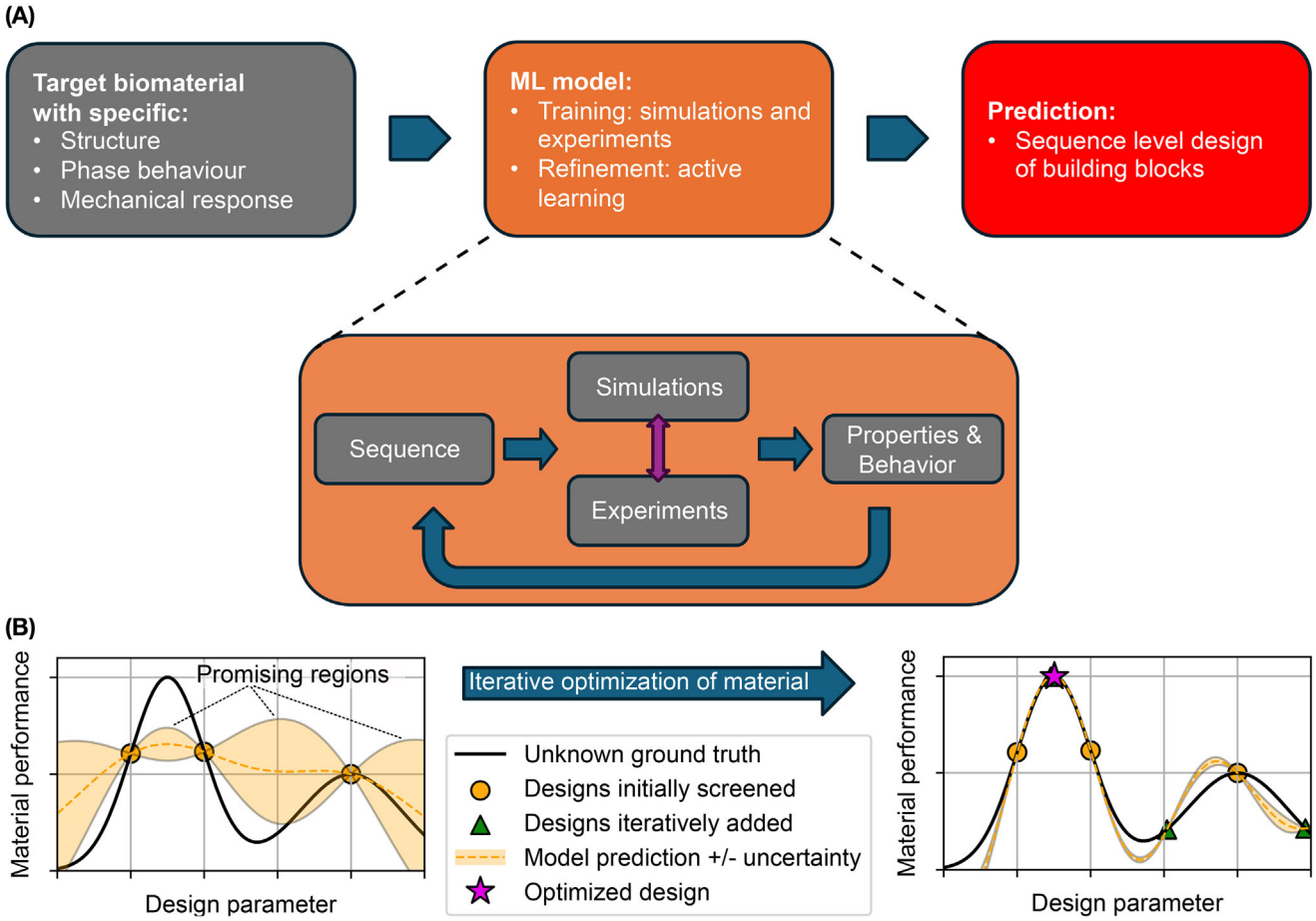

Figure 6. Outline for computationally guided design of DNA-based biomaterials. A) This workflow starts by defining the desired structure, phase behavior and mechanical response of DNA-based biomaterials. A machine-learning model trained on a dataset of simulations and experiments is then used to predict DNA building block design at the sequence level. During training, building blocks with different sequences are used to generate a library of emerging properties and behavior. Training could involve both simulations and experiments, with the option to couple both for efficient exploration of the parameter space. The ML model is trained to solve the inverse problem of predicting which sequence design led to the observed properties and behavior. B) During inference, the trained model predicts the sequence of building blocks. Active learning then augments the training data in design regions of high predicted material performance (exploitation) and/or high uncertainty (exploration). The example used a Gaussian process model with Bayesian optimization, but other architectures are feasible.

reduction in DNA synthesis costs will be critical for combining methods synergistically. In related fields, such as protein structure prediction, benchmarking is recognized as a crucial step to ensure that ML predictions are reliable.[168–170] Initiatives like the Materials Genome Initiative (MGI)[171,172] and efforts to establish electronic lab notebooks[173–175] emphasize the role of standardized data exchange methods, metadata specifications, and uncertainty quantification for materials data and modeling. Thus, we believe that data-driven, inverse design of DNA-based materials will become feasible with integrative approaches, putting new applications on the map that exploit control of complex material features.

4. DNA-Based Biomimetic Systems and Information Processing Materials

In this section, we focus on a selection of emerging and future applications with an overarching theme of DNA as a programmable material. Three promising areas, namely biomimetic testbeds, information processing based on addressable droplets, and mechanical computing are discussed in detail (Figure 2E–G). We envision that further development in these areas will be accelerated by integrating simulations, experiments and data-driven inverse design.

4.1. DNA Nanomotifs as Building Blocks For Biomimetic Condensates

DNA nanomotifs provide a programmable platform to test operation principles of living systems (**Figure 7**). For example, nanomotifs may be used to design biomimetic condensates.[12] In cells, biomolecular condensates contribute to subcellular organization and a variety of biological functions, such as transcription control.[176–178] The proteins comprising these cellular condensates organize into networks via transient

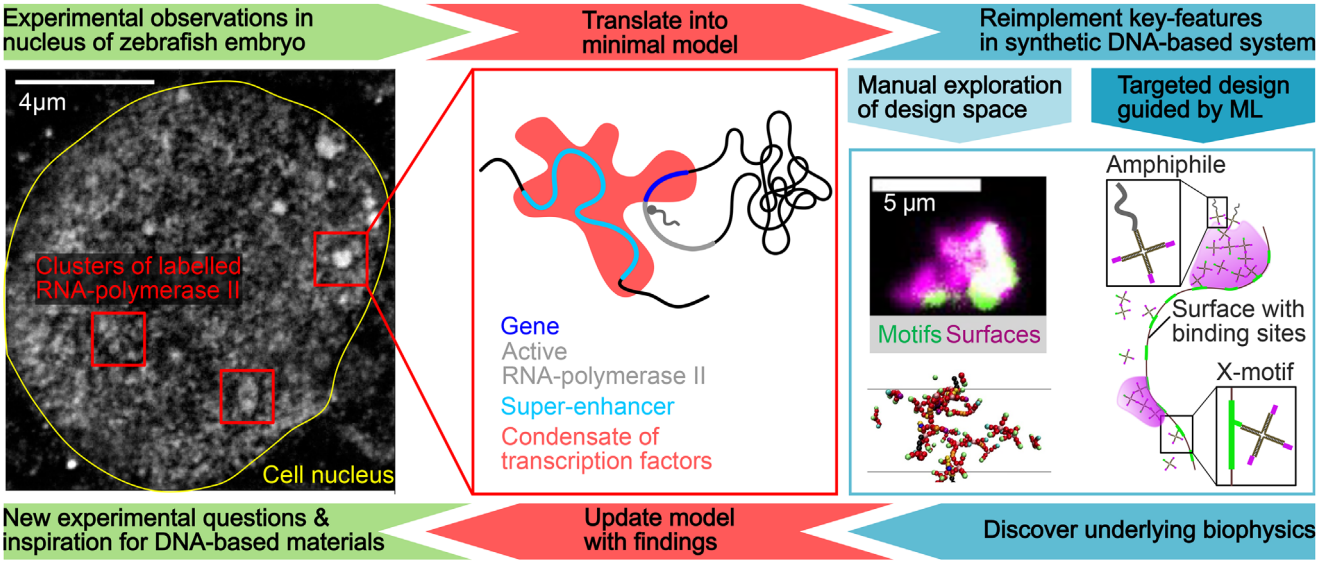

Figure 7. Biomimetic condensates: condensates of transcription factors are found in embryonic stem cells, e.g., from zebrafish. In a minimal model, surface condensation on super-enhancer sections of chromatin establishes the condensate. The condensate can be deformed by active transcription. Key features of this model have been reimplemented previously using DNA nanomotifs.[12] Current work focuses on including additional details, e.g., surfaces, into the synthetic reimplementation.[13] Simulations screen for promising building block designs and help explain observations at sequence level. Insights from the highly controlled synthetic system will refine the original model and help identify relevant questions for future experimental investigation. The acquired knowledge may also serve as inspiration for other DNA-based applications in information storage and processing. Data and code to detect clusters in stimulated emission double depletion (STEDD) microscopy images deposited with ref. [184]. Simulation snapshot generated with VMD.[132] Sketches of surface condensation adapted from ref. [13] under a CC BY license, Copyright 2025, the authors, published by Wiley Periodicals LLC.

multivalent interactions, typically emerging from a sticker-spacer architecture. Stickers (often intrinsically disordered regions or IDRs) form transient links with other stickers and are separated by spacers (folded domains) that interact with the solvent and provide structure.[179,180] Directly connecting biophysical properties of condensates to the amino acid sequence of proteins requires costly computational approaches and elaborate experiments based on expression of modified proteins in advanced in vivo or in vitro studies.[181–183]

DNA nanomotifs provide a similar sticker-spacer architecture via single-stranded sticky ends and double-stranded, structural parts. Since the nanomotifs are purely DNA-based, the number and strength of interaction sites, as well as motif structure can be programmed by defining sequences. Due to its specificity, connecting sequence design to emergent network properties is computationally tractable and, importantly, experimental validation can be accelerated. Single strands are commercially available and self-assemble into motifs, without the need for a complex expression system. The connection between sticker-spacer architecture of the nanomotif and emergence of phase-separation could be addressed in a targeted fashion by using ML-guided exploration of the nanomotif design space, as outlined in section 3.3. For example, one could systematically link phase behavior and condensate properties observed in vivo with generic sticker-spacer architectures.

Exemplifying the potential of biomimetic nanomotif systems, a computationally aided approach was used to explore the suspected role of amphiphilic RNA polymerase in the dispersal of transcriptional condensates.[12] Creating condensates of DNA nanomotifs and adding increasing concentrations of an amphiphilic nanomotif recreated changes in condensate shape, size and number observed in cellular transcriptional condensates. Amphiphilic nanomotifs also influenced non-equilibrium condensate properties in a time-resolved experiment: while the addition of nanomotifs led to continued growth and rounding of condensates over time, the addition of amphiphilic nanomotifs induced rounding but prevented growth, and ultimately dispersed the condensates.

Future extensions may include the use of DNA strands as surfaces to model the combined effect of amphiphile and surface interaction on condensate properties.[13] It has been shown that surface condensation on chromatin leads to the site-specific formation of condensates at sub-saturated concentrations.[183–186] Incorporating this mechanism into a synthetic system will provide a bottom-up perspective with precise control over number, spacing and strength of interaction sites on the surface.

Active, non-equilibrium biochemical processes can also be included into DNA-based condensates. Reaction-diffusion processes were used to create complex spatio-temporal responses in condensates of nanomotifs, which mimic those found in cells or within membraneless organelles, e.g., nucleoli.[19,21] Control over the dynamic compartmentalization inside condensates was demonstrated through strand-displacement reactions that could be arrested via a stop strand, creating a structured, functional internal environment.[19] Figure 7 summarizes the conceptual steps from in vivo experimental observations to a condensate model that is validated and updated by reimplementing key features in a synthetic, DNA-based system.

Biomimetic condensates will help us understand how cellular condensates, shaped by evolution, facilitate biological

functions. Insights into functional, cellular materials may then serve as inspiration for synthetic, DNA-based solutions for storage and processing of information, such as addressable condensates of DNA nanomotifs.

4.2. Addressable Nanomotif Droplets for Control of Reactions and Logic Operations

An "address-based system" in the context of DNA sequences refers to a design where specific molecular interactions are guided by unique DNA-sequence motifs, allowing precise targeting and control over reactions within a synthetic environment.[187] In this system, droplets of DNA nanomotifs act as reaction volumes that sequester functional molecules, while other droplets represent distinct targets that can be selectively addressed based on their unique DNA sequences, akin to DNA barcoding. By tuning nanomotif structure and sticky end sequences, such an address system would ensure specificity, enable scalability to numerous target droplets, and allow reversible interactions.

Experimental studies on DNA-sequence interactions, supported by simulations, provide a foundational understanding for developing address-based systems in synthetic biology.[188] The specificity of DNA-sequence interactions unlocks a range of applications: for example, programmable molecular computing circuits, where logical operations are conducted via sequence-specific interactions.[189,190] Another promising application lies in targeted drug-delivery platforms,[191] where therapeutic agents are sequestered within addressable DNA-based nanodroplets, and selectively released upon reaching specific cellular environments. Addressable droplets of nanomotifs that sequester and spatially separate different molecules, as demonstrated for cargoes of DNA and streptavidin,[192] will enable precise control over chemical reactions by targeted fusing of droplets, which then exchange their contents. Furthermore, reactions are accelerated by localizing the reactants to droplets. This was shown for transcription inside droplets, coupled to a downstream detection reaction.[193] Computation with droplets of DNA nanomotifs has also been demonstrated.[11] The authors used two nanomotif species that are initially mixed in a droplet via a bivalent linker nanomotif, but phase-separate once two miRNAs bind and cleave the linker motif. The production of two phase-separated droplet species thus constitutes the output of an AND-operation. This logic gate architecture was extended to recognize a pattern of 4 miRNAs that serve as tumor biomarker. This nanomotif system displayed non-equilibrium behavior, revealed through time-resolved imaging: the microscopic linker nanomotif valency was reduced over time by strand-displacement reactions, which affected the macroscopic phase behavior.

To ensure that nanomotifs phase-separate into droplets that then fuse or split in a controlled way, precise tuning of free energies associated with these processes is needed. oxDNA and similar models (Section 2.2) allow probing hybridization with explicit consideration of the 3D-structure of DNA and are well-suited to carry out this fine-tuning. Thus, a library of orthogonal sticky end addresses that have similar melting temperatures under the desired conditions may be created. Higher level coarse-grained models (Section 3.2) may then be used to investigate phase separation, fusion and fission of droplets to screen suitable designs for experimental implementation. ML (Section 3.3) holds the potential to accelerate such workflows by directly suggesting nanomotif designs and sticky end addresses, facilitating their implementation in biomedical and computational fields.

The nanomotifs forming addressable condensates could be conjugated to polymers, nanoparticles, proteins, and inorganic frameworks, adding enzymatic, mechanical, optical, or catalytic properties. Examples from the literature demonstrated covalent grafting of polymers to DNA nanomotifs, embedding metallic or semiconductor nanoparticles for optic and electronic functionalities, and interfacing with biomolecules to mimic or enhance biological functions.[127–130] A potential application enabled by conjugation with functional molecules and by precise control over phase behavior could be loading nanomotif droplets with different molecular cargoes that recognize the droplet addresses, as sketched in **Figure 8**. The droplets are then selectively fused by adding a linker nanomotif, enabling the cargoes to interact. The product of this controlled interaction, for instance an enzymatic modification, is then again stored in addressable droplets by adding a strand that splits the linker, preparing the system for further reaction steps. In essence, the addressable droplet system loads a molecular program, executes it and saves the output, providing an information processing platform that resembles the von Neumann architecture. In this architecture, a Central Processing Unit (CPU) dynamically connects to memory blocks on the basis of address codes, allowing selective reading and writing at shifting memory positions.[13]

Controlling the full free energy landscape of addressable nanomotif droplets could enable the construction of more complex circuits through selective and reversible interactions, enabling the execution of Boolean logic functions, memory storage, and information processing within a biomolecular framework. By using unique DNA sequences as molecular "addresses," logic gates and pathways may be created, allowing computations to occur autonomously within a self-contained system. This has the potential to enable decentralized, parallel computing processes directly within a biological or synthetic environment, complementing conventional silicon-based computing and harnessing the chemical specificity and programmability of DNA. To overcome constraints inherent to information transfer by slow and spatially undirected diffusion of molecules or droplets, one highly promising route is the embedding in cell-like nanoarchitectures,[194] including DNA-programmable scaffolds and condensates.[195,196] This type of computing "in native substrate" would enable the addition of smart control to the entire domain of biomedical technologies.

DNA address-based systems represent a key technological step toward practical DNA-computing platforms, which may eventually process information within living cells or perform complex analyses in diagnostic devices.

4.3. Using Sequence-Encoded Mechanics of DNA Networks for Information Storage and Processing

Information storage and processing may also be realized by using properties inherent to networked DNA materials. Using the sequence of DNA for synthetic data storage has recently gained significant attention for situations where biocompatibility,

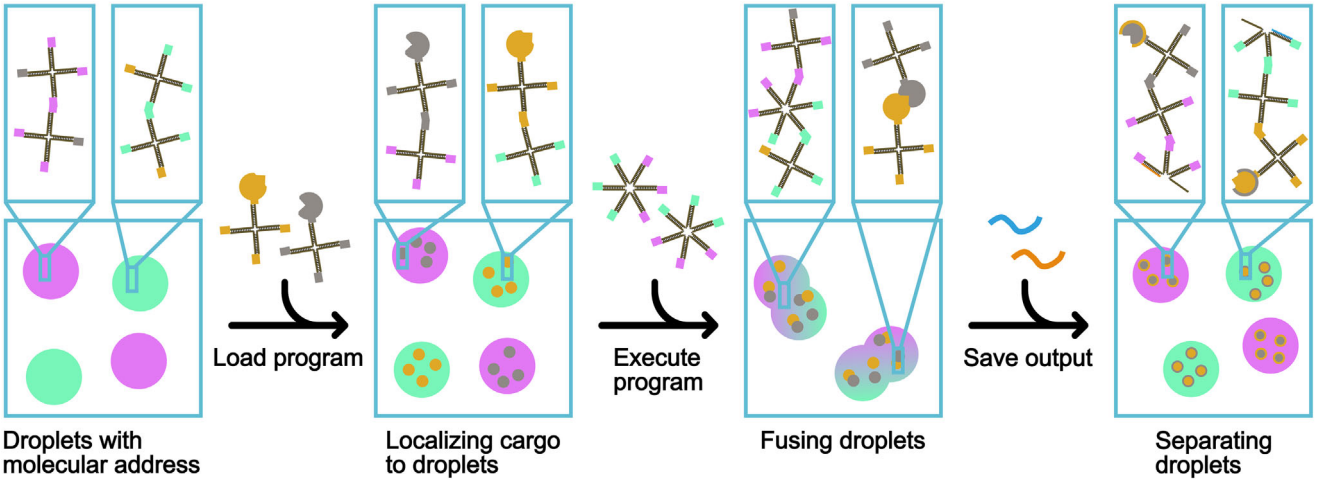

Figure 8. Reactions in addressable nanomotif droplets: two types of non-interacting nanomotif droplets are assembled, for instance through phase-separation or surface condensation on a DNA strand. The sticky end of the fourth arm in each nanomotif serves as molecular address. Molecules fused to nanomotifs can partition into droplets with the matching DNA sequence address, akin to loading a computer program into memory for parallel execution. A six-armed motif fuses the droplets, starting the program execution by allowing the cargo molecules to interact in a small reaction volume. A strand displacement reaction is then used to split the six-armed linker-nanomotif, separating the droplets and their cargo, thus saving the output of the reaction program.

sustainability, storage capacity or durability put traditional technologies at a disadvantage. For example, in dry air at 10°C, the estimated information retention time of DNA storage is on the order of $2 \cdot 10^7$ years.[197] Under conditions more relevant to DNA-based computing (aqueous solution at 20°C), this retention time would decrease to approximately 3400 years, which still surpasses the longevity of conventional flash memory. Furthermore, protocols for writing, storing, and retrieving data with error-correcting codes that include strategic redundancies have been demonstrated in the literature.[1,197–199] We envision that DNA will also be the basis for mechanical data storage and processing solutions, potentially in the form of mechanical computers.

Mechanical computing, with its roots deeply embedded in early mechanical devices used for calculations, is gaining renewed attention,[200] and offers an intriguing avenue for processing and storing data without relying solely on conventional electronic systems. We envision networks of DNA nanomotifs to function as programmable mechanical computers, given that their mechanical properties (Section 3.1) strongly depend on the sequence-level design of the motifs. For example, the network's viscoelasticity depends on the number of bases included in the sticky end segments that facilitate bridging between DNA nanomotifs. Enhancing or reducing the strength of DNA hydrogels is achieved by the inclusion of longer or shorter sticky ends, respectively. The incorporation of free joints or mismatches increases the flexibility of these networks, at the same time lowering their relative stiffness at fixed experimental conditions. These properties can be dynamically adapted through strand displacement reactions, changes in temperature or salt concentration.

This makes DNA networks well-suited to process and convert different input modalities (Figure 2G): for instance, by switching between mechanical states upon temperature changes, or the presence of a DNA strand that integrates into the network and modifies a mechanical readout. One application would be DNA/RNA sequence detection, as recently demonstrated using bulk rheology and microrheology.[20] Since microliter hydrogel volumes respond in a sequence-specific and dose-dependent manner, this method could offer real-time checks of gene integrity in a step preceding sequencing. Understanding the underlying sequence-property relationships could enable the development of portable biosensors, such as lateral flow assays, for rapid sequence-based diagnostics or detection of pathogens in blood or water samples.[20,201] Including temperature as a variable, **Figure 9** schematically describes our vision of how one can leverage the strong link between temperature and mechanical properties to use functional, thermally responsive DNA hydrogel systems as mechanical actuators that convey information encoded in the form of mechanical states. In this example, one provides heat as input to a functional material, here a DNA hydrogel. The hydrogel dynamically alters its mechanical state in response to a change in its environment. This conformational modification is registered mechanically, optically or electronically, e.g., through the use of micro-electromechanical systems (MEMS). These next-generation sensors may be designed to possess thermal capabilities, allowing them to almost simultaneously provide thermal input and transduce mechanical output (force or pressure).

To understand the microscopic origins of experimental readouts, one can use methods that allow scale bringing, for instance by connecting nucleotide-level simulations to models using bead-spring representations for simulating large networks (Section 3.2). Simulations and data-driven design may also aid in designing further mechanical elements, e.g., bistable systems,[202,203] origami-inspired structures or resonant beams out of DNA. Such structures may then be integrated with DNA-based address systems for execution of specific tasks, e.g., molecule sorting or mechanical signal transduction, at the nanoscale with high precision. Furthermore, DNA sequences can serve as "instructions" to guide nanoscale mechanical

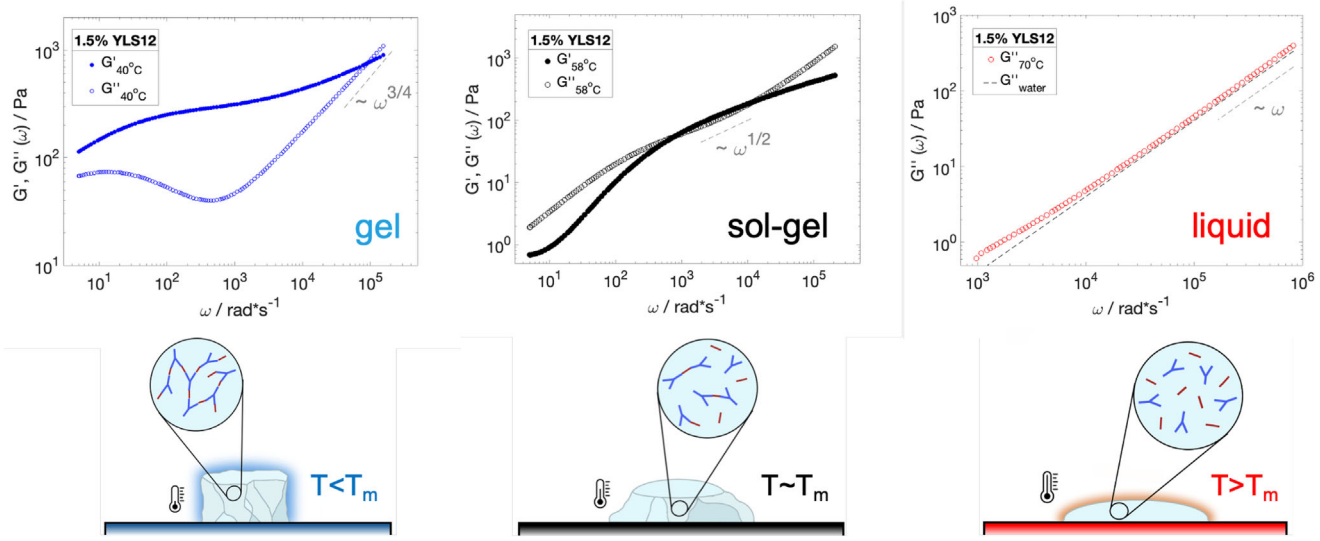

Figure 9. DWS measurement of mechanical output from a thermally responsive DNA system that could be used for information processing. Trivalent DNA nanomotifs were connected to fully complementary bivalent linkers with 12 nucleotides in their sticky ends to form a rigid hydrogel without any free bases (YLS12). Temperatures applied from left to right were 40°C, 58°C and 70°C. The high-level operation of this scheme relies on very sensitive temperature control and force/pressure sensing, which could be delivered by recent advances in micro-electromechanical systems (MEMS). Complicated logic circuits may then be built by the linking of individual DNA hydrogels comprised of different building blocks and controlled independently. Reproduced from ref. [20] under a CC BY license, Copyright 2025, the authors, published by John Wiley & Sons.

movements, enabling DNA nanostructures to function as molecular levers, hinges, and actuators.[204] Through the use of address-based targeting, these mechanical components can be selectively engaged to perform coordinated movements.

Thus, DNA nanomotif-based materials hold promise as multimodal sensors and biocompatible mechanical computers, provided that sequence-level design can be reliably linked to experimental readouts.

5. Conclusion

This perspective highlights promising advances of DNA-based materials for novel applications that address present-day technological challenges. Driven by the synergy between computational and experimental techniques, these applications are enabled by the tight link between sequence, structure, properties and behavior in DNA materials. We view DNA nanomotifs as molecular units holding sequence-dependent information that can be programmed and tailored via multiscale and ML approaches, illustrating the potential of using sequence-property relationships for functional material design. We discuss the strengths and limitations of atomistic and CG simulations, explore the complex behavior emerging from networks of programmable DNA nanomotifs, and review how thermodynamic and mechanical properties can be experimentally quantified. Integrative approaches, combining simulations at different scales with experiments for validation and detailed analysis of mesoscopic properties, can bridge our understanding of DNA at nucleotide level or below to properties and behavior emerging at micrometer scale of hydrogels and condensates. ML is poised to accelerate and streamline this process by enabling systematic optimization of simulation parameters, which we demonstrate with a Bayesian optimization strategy to fine-tune parameters of a CG model for DNA nanomotifs. Examples from the literature demonstrate how current methods enable the fabrication and characterization of materials with diverse properties, including phase separation, tunable viscoelasticity, reconfigurability, and responsiveness. As a future perspective, we anticipate that emerging integrative approaches – drawing inspiration from related areas of materials science – will establish quantitative links between these macroscopic observations and the underlying DNA sequence design. Predictive ML trained on data obtained with such scale-bringing approaches and active learning strategies could enable efficient design workflows, producing new functional materials. Standardized protocols, benchmarks and large-scale material libraries are a crucial next step to transform DNA nanomotif research into a scalable, predictable materials platform. We envision applications in biomimetic systems and biocompatible storage and processing of information, interfaced with mechanical and biochemical input and output. We believe the growing interest in programmable DNA-based materials will drive innovation and advance key applications outlined in this article.

Acknowledgements

The authors thank Xenia Tschurikow and Barbara Becker for experimental work, images and sketches related to surface condensation of nanomotifs. The authors thank Pascal Friederich for helpful discussions and providing code for parts of the Gaussian process model. This work was supported by the Helmholtz Association Program "Natural, Artificial, and Cognitive Information Processing" as well as the Networking Fund providing the HAICORE@KIT partition. The project was made possible by funding from the Carl-Zeiss-Stiftung and Center SynGen. EAOZ and IDS are supported by the Karlsruhe Institute of Technology Excellence Strategy via the Young Investigator Group Preparation Program.

Open access funding enabled and organized by Projekt DEAL.

Conflict of Interest

The authors declare no conflict of interest.

Data Availability Statement

All code used in Section 3.2 as well as angle distributions from oxDNA simulations and optimized parameters for ReaDDy simulations can be found on GitHub (https://github.com/aaron-gad/DNA_Nanomotif_ML_MD).

Keywords

biomimetic materials, DNA materials, DNA nanomotifs, information processing, machine learning, multiscale modeling

Received: July 28, 2025
Revised: September 12, 2025
Published online:

[1] A. Doricchi, C. M. Platnich, A. Gimpel, F. Horn, M. Earle, G. Lanzavecchia, A. L. Cortajarena, L. M. Liz-Marzán, N. Liu, R. Heckel, R. N. Grass, R. Krahne, U. F. Keyser, D. Garoli, *ACS Nano* **2022**, *16*, 17552.
[2] N. C. Seeman, *J. Theor. Biol.* **1982**, *99*, 237.
[3] P. W. Rothemund, *Nature* **2006**, *440*, 297.
[4] P. Zhan, A. Peil, Q. Jiang, D. Wang, S. Mousavi, Q. Xiong, Q. Shen, Y. Shang, B. Ding, C. Lin, Y. Ke, N. Liu, *Chem. Rev.* **2023**, *123*, 3976.
[5] K. Jahnke, M. Illig, M. Scheffold, M. P. Tran, U. Mersdorf, K. Göpfrich, *Adv. Funct. Mater.* **2024**, *34*, 2301176.
[6] N. C. Seeman, *Nanobiotechnol. Protoc.* **2005**, 143.
[7] S. H. Um, J. B. Lee, N. Park, S. Y. Kwon, C. C. Umbach, D. Luo, *Nat. Mater.* **2006**, *5*, 797.
[8] S. Biffi, R. Cerbino, F. Bomboi, E. M. Paraboschi, R. Asselta, F. Sciortino, T. Bellini, *Proc. Natl. Acad. Sci. USA* **2013**, *110*, 15633.
[9] H. Udono, J. Gong, Y. Sato, M. Takinoue, *Adv. Biol.* **2023**, *7*, 2200180.
[10] M. Takinoue, *Interface Focus* **2023**, *13*, 20230021.
[11] J. Gong, N. Tsumura, Y. Sato, M. Takinoue, *Adv. Funct. Mater.* **2022**, *32*, 2202322.
[12] X. Tschurikow, A. Gadzekpo, M. P. Tran, R. Chatterjee, M. Sobucki, V. Zaburdaev, K. Göpfrich, L. Hilbert, *Nano Lett.* **2023**, *23*, 7815.
[13] L. Hilbert, A. Gadzekpo, S. L. Vecchio, M. Wellhäusser, X. Tschurikow, R. Prizak, B. Becker, S. Burghart, E. A. Oprzeska-Zingrebe, *Ann. N. Y. Acad. Sci.* **2025**, *1552*, 12.
[14] E. Poppleton, J. Bohlin, M. Matthies, S. Sharma, F. Zhang, P. Šulc, *Nucleic Acids Res.* **2020**, *48*, e72.
[15] J. Bohlin, M. Matthies, E. Poppleton, J. Procyk, A. Mallya, H. Yan, P. Šulc, *Nat. Protoc.* **2022**, *17*, 1762.
[16] R. A. Brady, N. J. Brooks, P. Cicuta, L. Di Michele, *Nano Lett.* **2017**, *17*, 3276.
[17] B. Saccà, C. M. Niemeyer, *Chem. Soc. Rev.* **2011**, *40*, 5910.
[18] Q.-H. Zhao, F.-H. Cao, Z.-H. Luo, W. T. Huck, N.-N. Deng, *Angew. Chem.* **2022**, *134*, e202117500.
[19] A. Leathers, M. Walczak, R. A. Brady, A. Al Samad, J. Kotar, M. J. Booth, P. Cicuta, L. Di Michele, *J. Am. Chem. Soc.* **2022**, *144*, 17468.
[20] A. E. Can, A. W. Ali, C. Oelschlaeger, N. Willenbacher, I. D. Stoev, *Macromol. Rapid Commun.* **2025**, 2500149.
[21] J. Bucci, L. Malouf, D. A. Tanase, N. Farag, J. R. Lamb, R. Rubio-Sánchez, S. Gentile, E. Del Grosso, C. F. Kaminski, L. Di Michele, F. Ricci, *J. Am. Chem. Soc.* **2024**, *146*, 31529.
[22] J. SantaLucia, H. T. Allawi, P. A. Seneviratne, *Biochemistry* **1996**, *35*, 3555.
[23] Z. Xing, A. Caciagli, T. Cao, I. Stoev, M. Zupkauskas, T. O'Neill, T. Wenzel, R. Lamboll, D. Liu, E. Eiser, *Proc. Natl. Acad. Sci. USA* **2018**, *115*, 8137.
[24] N. Conrad, T. Kennedy, D. K. Fygenson, O. A. Saleh, *Proc. Natl. Acad. Sci. USA* **2019**, *116*, 7238.
[25] I. D. Stoev, T. Cao, A. Caciagli, J. Yu, C. Ness, R. Liu, R. Ghosh, T. O'Neill, D. Liu, E. Eiser, *Soft Matter* **2020**, *16*, 990.
[26] J. N. Zadeh, C. D. Steenberg, J. S. Bois, B. R. Wolfe, M. B. Pierce, A. R. Khan, R. M. Dirks, N. A. Pierce, *J. Comput. Chem.* **2011**, *32*, 170.
[27] F. Zaccaria, C. Fonseca Guerra, *Chem. - Eur. J.* **2018**, *24*, 16315.
[28] J. Yoo, D. Winogradoff, A. Aksimentiev, *Curr. Opin. Struct. Biol.* **2020**, *64*, 88.
[29] H. Kenzaki, S. Takada, *J. Mol. Biol.* **2021**, *433*, 166792.
[30] M. C. Zwier, L. T. Chong, *Curr. Opin. Pharmacol.* **2010**, *10*, 745.
[31] P. P. S. Russell, S. Alaeen, T. V. Pogorelov, *J. Phys. Chem. B* **2023**, *127*, 9863.
[32] G. Shahane, W. Ding, M. Palaiokostas, M. Orsi, *J. Molecular Model.* **2019**, *25*, 76.
[33] K. Sarthak, D. Winogradoff, Y. Ge, S. Myong, A. Aksimentiev, *J. Chem. Theory Comput.* **2023**, *19*, 3721.
[34] G. Alberini, S. A. Paz, B. Corradi, C. F. Abrams, F. Benfenati, L. Maragliano, *J. Chem. Theory Comput.* **2023**, *19*, 2953.
[35] M. M. Aboelnga, *Comput. Biol. Med.* **2022**, *146*, 105544.
[36] A. Pérez, F. J. Luque, M. Orozco, *Acc. Chem. Res.* **2012**, *45*, 196.
[37] K. Wu, C. Qi, Z. Zhu, C. Wang, B. Song, C. Chang, *J. Phys. Chem. Lett.* **2020**, *11*, 7002.
[38] G. Panda, A. Ray, *Int. J. Biol. Macromol.* **2024**, *283*, 137835.
[39] A. D. MacKerell Jr, J. Wiorkiewicz-Kuczera, M. Karplus, *J. Am. Chem. Soc.* **1995**, *117*, 11946.
[40] W. D. Cornell, P. Cieplak, C. I. Bayly, I. R. Gould, K. M. Merz, D. M. Ferguson, D. C. Spellmeyer, T. Fox, J. W. Caldwell, P. A. Kollman, *J. Am. Chem. Soc.* **1995**, *117*, 5179.
[41] K. Liebl, M. Zacharias, *Biophys. J.* **2023**, *122*, 2841.
[42] O. Love, R. Galindo-Murillo, M. Zgarbová, J. Sponer, P. Jurecka, T. E. Cheatham III, *J. Chem. Theory Comput.* **2023**, *19*, 4299.
[43] C. G. Ricci, J. S. Chen, Y. Miao, M. Jinek, J. A. Doudna, J. A. McCammon, G. Palermo, *ACS Cent. Sci.* **2019**, *5*, 651.
[44] B. Islam, P. Stadlbauer, A. Gil-Ley, G. Perez-Hernandez, S. Haider, S. Neidle, G. Bussi, P. Banas, M. Otyepka, J. Sponer, *J. Chem. Theory Comput.* **2017**, *13*, 2458.
[45] T. S. Alexiou, C. N. Likos, *J. Phys. Chem. B* **2023**, *127*, 6969.
[46] E. Routhier, A. Joubert, A. Westbrook, E. Pierre, A. Lancrey, M. Cariou, J.-B. Boulé, J. Mozziconacci, *Nucleic Acids Res.* **2024**, *52*, 6802.
[47] B. Mohr, T. van Heesch, A. P. de Alba Ortíz, J. Vreede, *Wiley Interdiscip. Rev.: Comput. Mol. Sci.* **2024**, *14*, e1712.
[48] V. Gapsys, B. L. de Groot, *J. Chem. Theory Comput.* **2017**, *13*, 6275.
[49] D. Farré-Gil, J. P. Arcon, C. A. Laughton, M. Orozco, *Nucleic Acids Res.* **2024**, *52*, 6791.
[50] F. Noé, A. Tkatchenko, K.-R. Müller, C. Clementi, *Annu. Rev. Phys. Chem.* **2020**, *71*, 361.
[51] S. Barissi, A. Sala, M. Wieczór, F. Battistini, M. Orozco, *Nucleic Acids Res.* **2022**, *50*, 9105.
[52] Z. Chen, L. Hu, B.-T. Zhang, A. Lu, Y. Wang, Y. Yu, G. Zhang, *Int. J. Mol. Sci.* **2021**, *22*, 3605.
[53] D. Elsing, W. Wenzel, M. Kozlowska, *J. Phys. Chem. B* **2025**, *129*, 1874.
[54] E. S. Kolesnikov, Y. Xiong, A. V. Onufriev, *J. Chem. Theory Comput.* **2024**, *20*, 8724.
[55] A. Madushanka, R. T. Moura Jr, N. Verma, E. Kraka, *Int. J. Mol. Sci.* **2023**, *24*, 6311.
[56] M. Wolter, M. Elstner, U. Kleinekathofer, T. Kubar, *J. Phys. Chem. B* **2017**, *121*, 529.

[57] P. Diamantis, I. Tavernelli, U. Rothlisberger, *J. Chem. Theory Comput.* **2020**, *16*, 6690.
[58] J. I. Mendieta-Moreno, D. G. Trabada, J. Mendieta, J. P. Lewis, P. Gomez-Puertas, J. Ortega, *J. Phys. Chem. Lett.* **2016**, *7*, 4391.
[59] J. J. Nogueira, S. Roßbach, C. Ochsenfeld, L. Gonzalez, *J. Chem. Theory Comput.* **2018**, *14*, 4298.
[60] P. D. Dans, J. Walther, H. Gómez, M. Orozco, *Curr. Opin. Struct. Biol.* **2016**, *37*, 29.
[61] Y. Sato, T. Sakamoto, M. Takinoue, *Sci. Adv.* **2020**, *6*, eaba3471.
[62] M. Soñora, L. H. Silva Santos, A. Alba, A. Ballesteros-Casallas, S. Pantano, *Wiley Interdiscip. Rev.: Comput. Mol. Sci.* **2025**, *15*, e70028.
[63] N. Korolev, D. Luo, A. P. Lyubartsev, L. Nordenskiöld, *Polymers* **2014**, *6*, 1655.
[64] C. Maffeo, T. T. Ngo, T. Ha, A. Aksimentiev, *J. Chem. Theory Comput.* **2014**, *10*, 2891.
[65] J. Kohler, Y. Chen, A. Kramer, C. Clementi, F. Noé, *J. Chem. Theory Comput.* **2023**, *19*, 942.
[66] T. E. Ouldridge, A. A. Louis, J. P. Doye, *Phys. Rev. Lett.* **2010**, *104*, 178101.
[67] T. E. Ouldridge, A. A. Louis, J. P. Doye, *J. Chem. Phys.* **2011**, *134*, 8.
[68] G. S. Freeman, D. M. Hinckley, J. P. Lequieu, J. K. Whitmer, J. J. De Pablo, *J. Chem. Phys.* **2014**, *141*, 16.
[69] Z.-C. Mu, Y.-L. Tan, J. Liu, B.-G. Zhang, Y.-Z. Shi, *Molecules* **2023**, *28*, 4833.
[70] B. E. Snodin, F. Randisi, M. Mosayebi, P. Šulc, J. S. Schreck, F. Romano, T. E. Ouldridge, R. Tsukanov, E. Nir, A. A. Louis, J. P. K. Doye, *J. Chem. Phys.* **2015**, *142*, 23.
[71] E. Poppleton, M. Matthies, D. Mandal, F. Romano, P. Šulc, L. Rovigatti, *J. Open Source Softw.* **2023**, *8*, 4693.
[72] L. Rovigatti, P. Šulc, I. Z. Reguly, F. Romano, *J. Comput. Chem.* **2015**, *36*, 1.
[73] E. Poppleton, R. Romero, A. Mallya, L. Rovigatti, P. Šulc, *Nucleic Acids Res.* **2021**, *49*, W491.
[74] Y. Hu, J. Rogers, Y. Duan, A. Velusamy, S. Narum, S. Al Abdullatif, K. Salaita, *Nat. Nanotechnol.* **2024**, *19*, 1674.
[75] V. Bukina, A. Božič, *Biophys. J.* **2024**, *123*, 3397.
[76] L. Yang, G. Pecastaings, C. Drummond, J. Elezgaray, *Nano Lett.* **2024**, *24*, 13481.
[77] X. Liu, F. Liu, H. Chhabra, C. Maffeo, Z. Chen, Q. Huang, A. Aksimentiev, T. Arai, *Nat. Commun.* **2024**, *15*, 7210.
[78] M. Mogheiseh, R. Hasanzadeh Ghasemi, *J. Chem. Phys.* **2024**, *161*, 4.
[79] R. Walker-Gibbons, X. Zhu, A. Behjatian, T. J. Bennett, M. Krishnan, *Sci. Rep.* **2024**, *14*, 20582.
[80] O. Henrich, Y. A. Gutiérrez Fosado, T. Curk, T. E. Ouldridge, *Eur. Phys. J. E* **2018**, *41*, 1.
[81] A. P. Thompson, H. M. Aktulga, R. Berger, D. S. Bolintineanu, W. M. Brown, P. S. Crozier, P. J. In't Veld, A. Kohlmeyer, S. G. Moore, T. D. Nguyen, R. Shan, M. J. Stevens, J. Tranchida, C. Trott, S. J. Plimpton, *Comput. Phys. Commun.* **2022**, *271*, 108171.
[82] L. Rovigatti, F. Bomboi, F. Sciortino, *J. Chem. Phys.* **2014**, *140*, 154903.
[83] A. Sengar, T. E. Ouldridge, O. Henrich, L. Rovigatti, P. Šulc, *Front. Mol. Biosci.* **2021**, *8*, 693710.
[84] M. Hoffmann, C. Fröhner, F. Noé, *PLoS Comput. Biol.* **2019**, *15*, e1006830.
[85] H. Ye, W. Xian, Y. Li, *ACS Omega* **2021**, *6*, 1758.
[86] H. Weeratunge, D. Robe, A. Menzel, A. W. Phillips, M. Kirley, K. Smith-Miles, E. Hajizadeh, *Rheol. Acta* **2023**, *62*, 477.
[87] A. Naserian-Nik, M. Tahani, M. Karttunen, *RSC Adv.* **2013**, *3*, 10516.
[88] J. Yoo, A. Aksimentiev, *Proc. Natl. Acad. Sci. USA* **2013**, *110*, 20099.
[89] L. V. Bock, M. Igaev, H. Grubmüller, *Curr. Opin. Struct. Biol.* **2024**, *86*, 102825.
[90] E. Natan, C. Baloglu, K. Pagel, S. M. V. Freund, N. Morgner, C. V. Robinson, A. R. Fersht, A. C. Joerger, *J. Mol. Biol.* **2011**, *409*, 358.
[91] M. R. Pradhan, J. W. Siau, S. Kannan, M. N. Nguyen, Z. Ouaray, C. K. Kwoh, D. P. Lane, F. Ghadessy, C. S. Verma, *Nucleic Acids Res.* **2019**, *47*, 1637.
[92] Q. Xu, M. Yang, J. Ji, J. Weng, W. Wang, X. Xu, *J. Chem. Inf. Model.* **2024**, *64*, 5219.
[93] E. A. Oprzeska-Zingrebe, J. Smiatek, *Phys. Chem. Chem. Phys.* **2021**, *23*, 1254.
[94] E. A. Oprzeska-Zingrebe, J. Smiatek, *J. Mol. Struct.* **2023**, *1274*, 134375.
[95] P. Stadlbauer, M. Krepl, T. E. Cheatham, J. Koča, J. Šponer, *Nucleic Acids Res.* **2013**, *41*, 7128.
[96] S. Cao, Q. Su, Y.-H. Chen, M.-L. Wang, Y. Xu, L.-H. Wang, Y.-H. Lu, J.-F. Li, J. Liu, X.-J. Hong, H.-Y. Wang, J.-P. Liu, Z.-G. Wang, *Int. J. Mol. Sci.* **2024**, *25*, 623.
[97] G. Fracchioni, S. Vailati, M. Grazioli, V. Pirota, *Molecules* **2024**, *29*, 3488.
[98] Y.-Y. Wu, L. Bao, X. Zhang, Z.-J. Tan, *J. Chem. Phys.* **2015**, *142*, 03B614_1.
[99] C. Maffeo, J. Yoo, A. Aksimentiev, *Nucleic Acids Res.* **2016**, *44*, 3013.
[100] K. Ahmad, A. Javed, C. Lanphere, P. V. Coveney, E. V. Orlova, S. Howorka, *Nat. Commun.* **2023**, *14*, 3630.
[101] J. J. Uusitalo, H. I. Ingolfsson, P. Akhshi, D. P. Tieleman, S. J. Marrink, *J. Chem. Theory Comput.* **2015**, *11*, 3932.
[102] G. Palombo, S. Weir, D. Michieletto, Y. A. Gutiérrez Fosado, *Nat. Mater.* **2025**, *24*, 454.
[103] N. Srinivas, T. E. Ouldridge, P. Šulc, J. M. Schaeffer, B. Yurke, A. A. Louis, J. P. Doye, E. Winfree, *Nucleic Acids Res.* **2013**, *41*, 10641.
[104] R. R. Machinek, T. E. Ouldridge, N. E. Haley, J. Bath, A. J. Turberfield, *Nat. Commun.* **2014**, *5*, 5324.
[105] L. Malouf, D. A. Tanase, G. Fabrini, R. A. Brady, M. Paez-Perez, A. Leathers, M. J. Booth, L. Di Michele, *Chem* **2023**, *9*, 3347.
[106] Y. Zhang, A. McMullen, L.-L. Pontani, X. He, R. Sha, N. C. Seeman, J. Brujic, P. M. Chaikin, *Nat. Commun.* **2017**, *8*, 21.
[107] J. Fernandez-Castanon, S. Bianchi, F. Saglimbeni, R. Di Leonardo, F. Sciortino, *Soft Matter* **2018**, *14*, 6431.
[108] L. G. Wilson, W. C. Poon, *Phys. Chem. Chem. Phys.* **2011**, *13*, 10617.
[109] U. Balucani, R. Vallauri, T. Gaskell, *Berichte der Bunsengesellschaft für physikalische Chemie* **1990**, *94*, 261.
[110] A. Kowalczyk, C. Oelschlaeger, N. Willenbacher, *Meas. Sci. Technol.* **2014**, *26*, 015302.
[111] C. Weis, C. Oelschlaeger, D. Dijkstra, M. Ranft, N. Willenbacher, *Sci. Rep.* **2016**, *6*, 33498.
[112] I. D. Stoev, A. Caciagli, Z. Xing, E. Eiser, in *Optical Trapping and Optical Micromanipulation XV*, vol. *10723*, SPIE, Bellingham, Washington, USA **2018**, pp. 251–262.
[113] I. D. Stoev, A. Mukhopadhyay, R. Tammen, E. Eiser, *Rheol. Acta* **2025**, *64*, 241.
[114] F. Català-Castro, S. Ortiz-Vásquez, C. Martínez-Fernández, F. Pezzano, C. Garcia-Cabau, M. Fernández-Campo, N. Sanfeliu-Cerdán, S. Jiménez-Delgado, X. Salvatella, V. Ruprecht, P.-A. Frigeri, M. Krieg, *Nat. Nanotechnol.* **2025**, *20*, 411.
[115] D. J. Pine, D. A. Weitz, J. Zhu, E. Herbolzheimer, *J. Phys.* **1990**, *51*, 2101.
[116] D. Weitz, J. Zhu, D. Durian, H. Gang, D. Pine, *Phys. Scr.* **1993**, *1993*, T49B610.
[117] K. Elsayad, G. Urstöger, C. Czibula, C. Teichert, J. Gumulec, J. Balvan, M. Pohlt, U. Hirn, *Cellulose* **2020**, *27*, 4209.
[118] R. Prevedel, A. Diz-Muñoz, G. Ruocco, G. Antonacci, *Nat. Methods* **2019**, *16*, 969.
[119] I. D. Stoev, M. Bolger-Munro, A. Minopoli, S. Wagner, V. R. Krishnaswamy, E. Erben, K. Weißenbruch, N. Maghelli, M. Bastmeyer, C.-P. Heisenberg, M. Kreysing, *bioRxiv* **2025**.

[120] P. Lemke, S. Moench, P. S. Jäger, C. Oelschlaeger, K. S. Rabe, C. M. Domínguez, C. M. Niemeyer, *Small Methods* **2024**, *8*, 2400251.
[121] M. Kamkar, R. Salehiyan, T. B. Goudoulas, M. Abbasi, C. Saengow, E. Erfanian, S. Sadeghi, G. Natale, S. A. Rogers, A. J. Giacomin, U. Sundararaj, *Prog. Polym. Sci.* **2022**, *132*, 101580.
[122] K. Hyun, M. Wilhelm, C. O. Klein, K. S. Cho, J. G. Nam, K. H. Ahn, S. J. Lee, R. H. Ewoldt, G. H. McKinley, *Prog. Polym. Sci.* **2011**, *36*, 1697.
[123] P. C. Cai, B. A. Krajina, M. J. Kratochvil, L. Zou, A. Zhu, E. B. Burgener, P. L. Bollyky, C. E. Milla, M. J. Webber, A. J. Spakowitz, S. C. Heilshorn, *Soft Matter* **2021**, *17*, 1929.
[124] S. K. Nandi, N. S. Gov, *Eur. Phys. J. E* **2018**, *41*, 117.
[125] E. Dieterich, J. Camunas-Soler, M. Ribezzi-Crivellari, U. Seifert, F. Ritort, *Nat. Phys.* **2015**, *11*, 971.
[126] J. Zhang, W. Zheng, S. Zhang, D. Xu, Y. Nie, Z. Jiang, N. Xu, *Sci. Adv.* **2021**, *7*, eabg6766.
[127] F. Li, D. Lyu, S. Liu, W. Guo, *Adv. Mater.* **2020**, *32*, 1806538.
[128] D. Cao, Y. Xie, J. Song, *Macromol. Rapid Commun.* **2022**, *43*, 2200281.
[129] J. Gačanin, C. V. Synatschke, T. Weil, *Adv. Funct. Mater.* **2020**, *30*, 1906253.
[130] D. Wang, Y. Hu, P. Liu, D. Luo, *Acc. Chem. Res.* **2017**, *50*, 733.
[131] M. A. Rad, H. Mahmodi, E. C. Filipe, T. R. Cox, I. Kabakova, J. L. Tipper, *Bioprinting* **2022**, *25*, e00179.
[132] W. Humphrey, A. Dalke, K. Schulten, *J. Mol. Graphics* **1996**, *14*, 33.
[133] S. Geggier, A. Kotlyar, A. Vologodskii, *Nucleic Acids Res.* **2011**, *39*, 1419.
[134] N. Theodorakopoulos, M. Peyrard, *Phys. Rev. Lett.* **2012**, *108*, 078104.
[135] P. I. Frazier, *arXiv* **2018**, https://doi.org/10.48550/arXiv.1807.02811.
[136] M. Balandat, B. Karrer, D. R. Jiang, S. Daulton, B. Letham, A. G. Wilson, E. Bakshy, in *Advances in Neural Information Processing Systems 33*, Vancouver, Canada **2020**.
[137] A. Paszke, S. Gross, F. Massa, A. Lerer, J. Bradbury, G. Chanan, T. Killeen, Z. Lin, N. Gimelshein, L. Antiga, A. Desmaison, A. Kopf, E. Yang, Z. DeVito, M. Raison, A. Tejani, S. Chilamkurthy, B. Steiner, L. Fang, J. Bai, S. Chintala, in *Advances in Neural Information Processing Systems 32*, Curran Associates, Inc. , New York **2019**, pp. 8024–8035.
[138] I. D. Stoev, A. Caciagli, A. Mukhopadhyay, C. Ness, E. Eiser, *Phys. Rev. E* **2021**, *104*, 054602.
[139] Z. Xing, C. Ness, D. Frenkel, E. Eiser, *Macromolecules* **2019**, *52*, 504.
[140] S. E. Farr, E. J. Woods, J. A. Joseph, A. Garaizar, R. Collepardo-Guevara, *Nat. Commun.* **2021**, *12*, 2883.
[141] H. I. Ingólfsson, H. Bhatia, F. Aydin, T. Oppelstrup, C. A. López, L. G. Stanton, T. S. Carpenter, S. Wong, F. Di Natale, X. Zhang, J. Y. Moon, C. B. Stanley, J. R. Chavez, K. Nguyen, G. Dharuman, V. Burns, R. Shrestha, D. Goswami, G. Gulten, Q. N. Van, A. Ramanathan, B. Van Essen, N. W. Hengartner, A. G. Stephen, T. Turbyville, P.-T. Bremer, S. Gnanakaran, J. N. Glosli, F. C. Lightstone, D. V. Nissley, et al., *J. Chem. Theory Comput.* **2023**, *19*, 2658.
[142] P. Kordt, J. J. Van Der Holst, M. Al Helwi, W. Kowalsky, F. May, A. Badinski, C. Lennartz, D. Andrienko, *Adv. Funct. Mater.* **2015**, *25*, 1955.
[143] Z. Wang, Z. Sun, H. Yin, X. Liu, J. Wang, H. Zhao, C. H. Pang, T. Wu, S. Li, Z. Yin, X.-F. Yu, *Adv. Mater.* **2022**, *34*, 2104113.
[144] J. F. Rodrigues, L. Florea, M. C. De Oliveira, D. Diamond, O. N. Oliveira, *Discov. Mater.* **2021**, *1*, 1.
[145] J. Wu, L. Torresi, M. Hu, P. Reiser, J. Zhang, J. S. Rocha-Ortiz, L. Wang, Z. Xie, K. Zhang, B.-W. Park, A. Barabash, Y. Zhao, J. Luo, Y. Wang, L. Lüer, L.-L. Deng, J. A. Hauch, D. M. Guldi, M. Eugenia Pérez-Ojeda, S. I. Seok, P. Friedrich, C. J. Brabec, *Science* **2024**, *386*, 1256.
[146] A. Ghafarollahi, M. J. Buehler, *Digital Discovery* **2024**, *3*, 1389.
[147] Y. Jin, P. V. Kumar, *Nanoscale* **2023**, *15*, 10975.
[148] Y. Zhang, D. W. Apley, W. Chen, *Sci. Rep.* **2020**, *10*, 4924.
[149] Y. Tian, T. Li, J. Pang, Y. Zhou, D. Xue, X. Ding, T. Lookman, *npj Comput. Mater.* **2025**, *11*, 209.
[150] V. Moro, C. Loh, R. Dangovski, A. Ghorashi, A. Ma, Z. Chen, S. Kim, P. Y. Lu, T. Christensen, M. Soljačić, *Newton* **2025**, *1*, 1.
[151] M. Manica, J. Born, J. Cadow, D. Christofidellis, A. Dave, D. Clarke, Y. G. N. Teukam, G. Giannone, S. C. Hoffman, M. Buchan, V. Chenthamarakshan, T. Donovan, H. H. Hsu, F. Zipoli, O. Schilter, A. Kishimoto, L. Hamada, I. Padhi, K. Wehden, L. McHugh, A. Khrabrov, P. Das, S. Takeda, J. R. Smith, *npj Comput. Mater.* **2023**, *9*, 69.
[152] E. O. Pyzer-Knapp, M. Manica, P. Staar, L. Morin, P. Ruch, T. Laino, J. R. Smith, A. Curioni, *npj Comput. Mater.* **2025**, *11*, 61.
[153] D. D. K. Wayo, *Arch. Comput. Meth. Eng.* **2025**, 1.
[154] A. M. Schweidtmann, D. Zhang, M. Von Stosch, *Digit. Chem. Eng.* **2024**, *10*, 100136.
[155] X. Jiang, H. Fu, Y. Bai, L. Jiang, H. Zhang, W. Wang, P. Yun, J. He, D. Xue, T. Lookman, Y. Su, J. Xie, *Adv. Funct. Mater.* **2025**, *35*, 2507734.
[156] Y. Kang, W. Lee, T. Bae, S. Han, H. Jang, J. Kim, *J. Am. Chem. Soc.* **2025**, *147*, 3943.
[157] Z. Yang, S. K. Yorke, T. P. Knowles, M. J. Buehler, *Sci. Adv.* **2025**, *11*, eadv1971.
[158] A. Ghafarollahi, M. J. Buehler, *arXiv* **2025**, https://doi.org/10.48550/arXiv.2504.19017.
[159] A. Ghafarollahi, M. J. Buehler, *Adv. Mater.* **2025**, *37*, 2413523.
[160] D. C. Elton, Z. Boukouvalas, M. D. Fuge, P. W. Chung, *Mol. Syst. Des. Eng.* **2019**, *4*, 828.
[161] Y. Liu, T. Zhao, W. Ju, S. Shi, *J. Materiomics* **2017**, *3*, 159.
[162] L. Chen, G. Pilania, R. Batra, T. D. Huan, C. Kim, C. Kuenneth, R. Ramprasad, *Mater. Sci. Eng. R Rep.* **2021**, *144*, 100595.
[163] K. Choudhary, B. DeCost, C. Chen, A. Jain, F. Tavazza, R. Cohn, C. W. Park, A. Choudhary, A. Agrawal, S. J. Billinge, E. Holm, S. P. Ong, C. Wolverton, *npj Comput. Mater.* **2022**, *8*, 59.
[164] S. A. Moench, P. Lemke, J. Weisser, I. D. Stoev, K. S. Rabe, C. M. Domínguez, C. M. Niemeyer, *Chem. - Eur. J.* **2024**, *30*, e202401788.
[165] Y.-H. Peng, S.-K. Hsiao, K. Gupta, A. Ruland, G. K. Auernhammer, M. F. Maitz, S. Boye, J. Lattner, C. Gerri, A. Honigmann, C. Werner, E. Krieg, *Nat. Nanotechnol.* **2023**, *18*, 1463.
[166] A. Cangialosi, C. Yoon, J. Liu, Q. Huang, J. Guo, T. D. Nguyen, D. H. Gracias, R. Schulman, *Science* **2017**, *357*, 1126.
[167] M. Seifermann, P. Reiser, P. Friederich, P. A. Levkin, *Small Methods* **2023**, *7*, 2300553.
[168] L. Dobson, G. E. Tusnády, P. Tompa, *Brief. Bioinform.* **2025**, *26*, bbaf104.
[169] Q. Le, F. Sievers, D. G. Higgins, *Bioinformatics* **2017**, *33*, 1331.
[170] E. F. McDonald, T. Jones, L. Plate, J. Meiler, A. Gulsevin, *Structure* **2023**, *31*, 111.
[171] J. J. De Pablo, B. Jones, C. L. Kovacs, V. Ozolins, A. P. Ramirez, *Curr. Opin. Solid State Mater. Sci.* **2014**, *18*, 99.
[172] J. J. de Pablo, N. E. Jackson, M. A. Webb, L.-Q. Chen, J. E. Moore, D. Morgan, R. Jacobs, T. Pollock, D. G. Schlom, E. S. Toberer, J. Analytis, I. Dabo, D. M. DeLongchamp, G. A. Fiete, G. M. Grason, G. Hautier, Y. Mo, K. Rajan, E. J. Reed, E. Rodriguez, V. Stevanovic, J. Suntivich, K. Thornton, J.-C. Zhao, *npj Comput. Mater.* **2019**, *5*, 41.
[173] N. CARP, A. Minges, M. Piel, *J. Open Source Softw.* **2017**, *2*, 146.
[174] P. Tremouilhac, A. Nguyen, Y.-C. Huang, S. Kotov, D. S. Lütjohann, F. Hübsch, N. Jung, S. Bräse, *J. cheminform.* **2017**, *9*, 54.
[175] S. G. Higgins, A. A. Nogiwa-Valdez, M. M. Stevens, *Nat. Protoc.* **2022**, *17*, 179.
[176] A. S. Lyon, W. B. Peeples, M. K. Rosen, *Nat. Rev. Mol. Cell Biol.* **2021**, *22*, 215.
[177] S. F. Banani, H. O. Lee, A. A. Hyman, M. K. Rosen, *Nat. Rev. Mol. Cell Biol.* **2017**, *18*, 285.

[178] L. Hilbert, Y. Sato, K. Kuznetsova, T. Bianucci, H. Kimura, F. Jülicher, A. Honigmann, V. Zaburdaev, N. L. Vastenhouw, *Nat. Commun.* **2021**, *12*, 1360.
[179] R. V. Pappu, S. R. Cohen, F. Dar, M. Farag, M. Kar, *Chem. Rev.* **2023**, *123*, 8945.
[180] T. Mittag, R. V. Pappu, *Mol. Cell* **2022**, *82*, 2201.
[181] K. L. Saar, D. Qian, L. L. Good, A. S. Morgunov, R. Collepardo-Guevara, R. B. Best, T. P. Knowles, *Chem. Rev.* **2023**, *123*, 8988.
[182] S. Alberti, A. Gladfelter, T. Mittag, *Cell* **2019**, *176*, 419.
[183] A. R. Strom, J. M. Eeftens, Y. Polyachenko, C. J. Weaver, H.-F. Watanabe, D. Bracha, N. D. Orlovsky, C. C. Jumper, W. M. Jacobs, C. P. Brangwynne, *Mol. Biol. Cell* **2024**, *35*, ar88.
[184] A. Pancholi, T. Klingberg, W. Zhang, R. Prizak, I. Mamontova, A. Noa, M. Sobucki, A. Y. Kobitski, G. U. Nienhaus, V. Zaburdaev, L. Hilbert, *Molecular Syst. Biol.* **2021**, *17*, e10272.
[185] T. Klingberg, I. Wachter, A. Pancholi, Y. Gohar, P. Kumar, M. Sobucki, E. Kämmer, S. Eroğlu-Kayıkçı, S. Erhardt, C. Ferrai, V. Zaburdaev, L. Hilbert, *bioRxiv* **2023**, 2023.
[186] J. A. Morin, S. Wittmann, S. Choubey, A. Klosin, S. Golfier, A. A. Hyman, F. Jülicher, S. W. Grill, *Nat. Phys.* **2022**, *18*, 271.
[187] K. N. Lin, K. Volkel, J. M. Tuck, A. J. Keung, *Nat. Commun.* **2020**, *11*, 2981.
[188] G. Gines, A. S. Zadorin, J.-C. Galas, T. Fujii, A. Estevez-Torres, Y. Rondelez, *Nat. Nanotechnol.* **2017**, *12*, 351.
[189] A. P. Lapteva, N. Sarraf, L. Qian, *J. Am. Chem. Soc.* **2022**, *144*, 12443.
[190] A. C. Bardales, V. Smirnov, K. Taylor, D. M. Kolpashchikov, *ChemBioChem* **2024**, *25*, 202400080.
[191] F. Mollarasouli, U. Badilli, N. K. Bakirhan, S. A. Ozkan, Y. Ozkan, *J. Drug Deliv. Sci. Tec.* **2021**, *61*, 102290.
[192] B.-j. Jeon, D. T. Nguyen, O. A. Saleh, *J. Phys. Chem. B* **2020**, *124*, 8888.
[193] E. Kengmana, E. Ornelas-Gatdula, K.-L. Chen, R. Schulman, *J. Am. Chem. Soc.* **2024**, *146*, 32942.
[194] A. Joesaar, S. Yang, B. Bögels, A. van der Linden, P. Pieters, B. V. V. S. Kumar, N. Dalchau, A. Phillips, S. Mann, T. F. A. de Greef, *Nat. Nanotechnol.* **2019**, *14*, 369.
[195] G. Chatterjee, N. Dalchau, R. A. Muscat, A. Phillips, G. Seelig, *Nat. Nanotechnol.* **2017**, *12*, 920.
[196] S. Do, C. Lee, T. Lee, D. N. Kim, Y. Shin, *Sci. Adv.* **2022**, *8*, eabj1771.
[197] V. Zhirnov, R. M. Zadegan, G. S. Sandhu, G. M. Church, W. L. Hughes, *Nat. Mater.* **2016**, *15*, 366.
[198] C. Zhang, R. Wu, F. Sun, Y. Lin, Y. Liang, J. Teng, N. Liu, Q. Ouyang, L. Qian, H. Yan, *Nature* **2024**, *634*, 824.
[199] L. C. Meiser, P. L. Antkowiak, J. Koch, W. D. Chen, A. X. Kohll, W. J. Stark, R. Heckel, R. N. Grass, *Nat. Protoc.* **2020**, *15*, 86.
[200] H. Yasuda, P. R. Buskohl, A. Gillman, T. D. Murphey, S. Stepney, R. A. Vaia, J. R. Raney, *Nature* **2021**, *598*, 39.
[201] P. Xu, T. Cao, Q. Fan, X. Wang, F. Ye, E. Eiser, *Proc. Natl. Acad. Sci. USA* **2023**, *120*, e2305995120.
[202] C. K. Wong, J. P. Doye, *Appl. Sci.* **2022**, *12*, 5875.
[203] W. T. Kaufhold, W. Pfeifer, C. E. Castro, L. Di Michele, *ACS nano* **2022**, *16*, 8784.
[204] Q. Zhang, S. Xu, J. Zheng, J.-R. Zhang, J.-J. Zhu, *iScience* **2023**, *26*, 106327.